CHALMERS
UNIVERSITY OF TECHNOLOGY

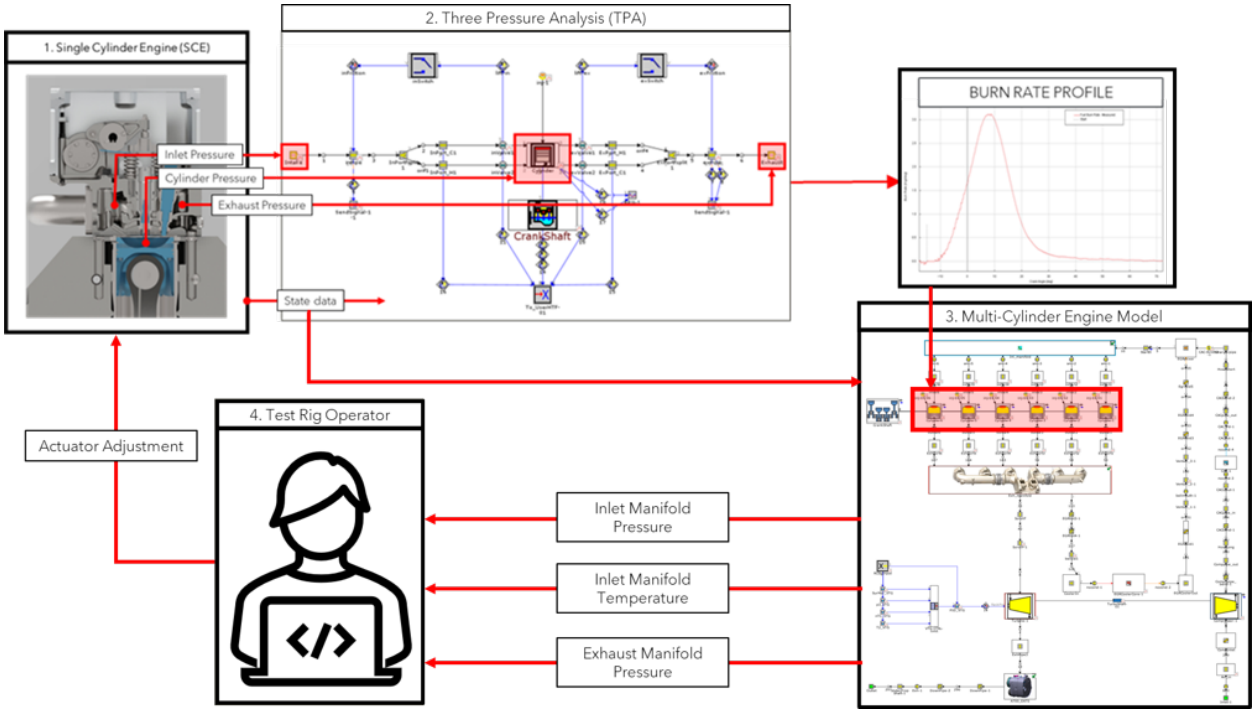

Virtual Multi-Cylinder Engine

Experimental and simulation data "in loop" towards a "virtual multi-cylinder engine" for pre-mixed hydrogen combustion

Master's thesis in Mechanics and Maritime Science

Mohammad Rusail Karattuthodi
Theodore Pierce Repinz

DEPARTMENT OF MECHANICS AND MARITIME SCIENCE
CHALMERS UNIVERSITY OF TECHNOLOGY
Gothenburg, Sweden 2026
www.chalmers.se

Master's thesis 2026

Virtual Multi-Cylinder

Experimental and simulation data "in loop" towards a "virtual multi-cylinder engine" for pre-mixed hydrogen combustion

Mohammad Rusail Karattuthodi

Theodore Pierce Repinz

CHALMERS
UNIVERSITY OF TECHNOLOGY

Chalmers University of Technology
Department of Mechanics and Maritime Sciences
Volvo Group
Department of Powertrain Engineering
Gothenburg, Sweden 2026

Virtual Multi-Cylinder Engine
Mohammad Rusail Karattuthodi
Theodore Pierce Repinz

Supervisor: Alaleh Safari, Volvo, Powertrain Strategic Development
Supervisor: Djordje Purkovic, Volvo, Powertrain Strategic Development
Supervisor: Elvin Zanjani, Chalmers University, Mechanics and Maritime Sciences
Supervisor: Erik Svensson, Volvo, Engine Performance and Simulation
Supervisor: Jan Eismark, Volvo, Powertrain Strategic Development
Supervisor: Jian Zhu, Volvo, Combustion System and Simulation
Examiner: Petter Dehlander, Department of Mechanics and Maritime Sciences

Master's Thesis 2026
Department of Mechanics and Maritime Sciences
Chalmers University of Technology
SE-412 96 Gothenburg
Telephone +46 31 772 1000

Cover: Virtual 0D/1D multi-cylinder engine "loop".

Typeset in LaTeX
Printed by Chalmers Reproservice
Gothenburg, Sweden 2026

Abstract

This project introduces an integrated methodology and tool set that couples experimental data from a single-cylinder engine (SCE) with a 0D/1D Three-Pressure-Analysis (TPA) model and a multi-cylinder engine (MCE) simulation in GT-Suite. The system developed utilizes measured data from a SCE and uses this to compute an apparent burn rate in a TPA model. This apparent burn rate, along with other operational data is extracted from the SCE and imposed onto a 0D/1D MCE simulation environment where the feedback is a set of boundary conditions corresponding to the inlet and exhaust manifold of the MCE. These boundary conditions are then used to adjust actuators on the SCE - enabling the continuation of a closed loop system until boundary condition convergence criteria have been met.

This concept addressed the two main shortcomings of SCE testing and 0D/1D simulation, respectively. In SCE testing, the entire engine system is decoupled, and each subsystem can be controlled independently for a specific load point. This implies that only steady state operation is possible, while the data that is collected is high fidelity measurement directly from the engine. A 0D/1D MCE simulation can model the system-level engine response, however in the context of premixed hydrogen engines, the combustion models are not mature enough to accurately represent in-cylinder combustion events.

The integration of a TPA-derived burn rate into the 0D/1D MCE model allowed the gap to be bridged between simplified simulation and experimental reality. A symbiotic looped workflow was established, and this paper shows that there exists potential to optimize the design quality and time of high-performance MCE concepts for future powertrain development.

A data sampling and averaging study was conducted to understand how the output of the simulation components reacted to cyclic variations. The study showed that key performance parameters are not significantly affected by the sample size when compared to a 200-cycle average; however are more sensitive to the sampling window - suggesting a sensitivity to cyclic variations. A minimum of 50 averaged cycles is required for accurate system results.

Furthermore, the output of an initial loop iteration of the 'virtual MCE' simulation tool is compared to a similar experimental MCE as a means to understand the system's initial conditions and validate the concept. This investigation was inconclusive, and hardware discrepancies were found to be evident in the test setups.

The continuation of loop iterations was halted by the lack of access to a dedicated SCE test bed. The initial iteration found absolute inlet manifold boundary condition errors of 7.14% for pressure, and 82.4% for temperature. While the absolute exhaust manifold back pressure error was found to be 3.98%.

The overarching research question was found to be inconclusive. However, this report sets the foundation for future work and discusses how further research can be conducted to aid in realizing its successful outcome. This thesis offers a set of recommendations for continued progression in realizing this as an industry tool. The thesis was therefore written in a manner to aid in future work and can be used as reference for configuring simulation models, addressing errors in future studies and is useful reference for relevant theory.

Keywords: Internal Combustion Engines, Hydrogen Combustion, Three Pressure Analysis, 0D/1D Simulation.

Acknowledgments

Our deepest thanks go to our families and friends, whose constant support and sacrifices have allowed us to be a part of this work at Chalmers University of Technology and Volvo Group. We are eternally grateful for the foundation that made this journey possible.

To our supervisors, thank you for sharing your expertise and for your tireless guidance as we navigated the challenges of powertrain engineering and development. We are honored by the time and patience you invested in our growth, and we carry the lessons learned here with immense gratitude.

List of Acronyms

Below is the list of acronyms that have been used throughout this thesis listed in alphabetical order:

AFR	Air Fuel Ratio
BMEP	Brake Mean Effective Pressure
CA50	50% Mass Fraction Burned
CO_2	Carbon Dioxide
CO	Carbon Monoxide
CoV	Coefficient of Variance
CoV_{IMEP}	Coefficient of Variation of Indicated Mean Effective Pressure
CFD	Computational Fluid Dynamics
DI	Direct Injection
DSL	Data Science Lab
EGR	Exhaust Gas Recirculation
EOE	End of Energizing
FRM	Fast Running Models
GT	Gamma Technologies
H2ICE	Hydrogen Internal Combustion Engines
HC	Hydrocarbon
HCCI	Homogeneous Charge Compression Ignition
ICE	Internal Combustion Engine
IVC	Intake Valve Closing
IMEP	Indicated Mean Effective Pressure
ISO	International Organization for Standardization
KIT	Karlsruhe Institute of Technology
LPDI	Low Pressure Direct Injection
MCE	Multi Cylinder Engine
NO_x	Nitrous Oxides
OEM	Original Equipment Manufacturers
PFI	Port Fuel Injection
PID	Proportional Integral Derivative (controller)
SCE	Single Cylinder Engine
SI	Spark Ignition
SOE	Start of Energizing
TPA	Three Pressure Analysis
VGT	Variable Geometry Turbo

Nomenclature

Below is the nomenclature of indices, sets, parameters, and variables that have been used throughout this thesis.

Parameters

P_{in}	Inlet boundary pressure
P_{exh}	Exhaust boundary pressure
T_{in}	Inlet boundary temperature

Variables

m_u	Unburned zone mass
$m_{f,b}$	Fuel mass transferred to burned zone
$m_{a,b}$	Air mass transferred to burned zone
$m_{f,i}$	Injected fuel mass
e_u	Unburned zone energy
p	Cylinder pressure
V_u	Unburned zone volume
h_f	Enthalpy of fuel mass
h_a	Enthalpy of air mass
$h_{f,i}$	Enthalpy of injected fuel mass
Q_u	Unburned zone heat transfer rate

m_b	Burned zone mass
$m_{f,b}$	Fuel mass transferred to burned zone
$m_{a,b}$	Air mass transferred to burned zone
e_b	Burned zone energy
p	Cylinder pressure
v_b	Burned zone volume
h_f	Bnthalpy of fuel mass
h_a	Bnthalpy of air mass
Q_b	burned zone heat transfer rate

Contents

List of Figures

List of Tables

1
Introduction

1.1 Background

Internal Combustion Engines (ICE) play a crucial role in the transportation industry. The sector remains a major contributor to greenhouse gas emissions, with most of the fuel currently in use being fossil fuels. In response, the European Union has committed to achieving carbon neutrality by 2050, which demands a significant reduction in emissions from fossil fuel combustion. Using alternative fuels with low or no carbon content is one solution to reduce the CO_2 emissions from ICEs.

Hydrogen is one such promising alternative fuel that has zero carbon content. During hydrogen combustion, the primary emissions are NO_x along with water in liquid and vapor forms [13]. Some key attributes of hydrogen fuel include a low ignition energy, a high diffusion coefficient, a high laminar flame speed, and a wide flammability range. The wide flammability range makes it suitable for lean operation, potentially resulting in increased engine efficiency due to the reduction in pumping losses and wall heat transfer [4]. However, due to the low ignition energy of hydrogen, abnormal combustion events like backfire and knock can become more prominent, potentially inhibiting the engine from reaching high power outputs. These abnormal combustion events are particularly hard to manage in pre-mixed hydrogen combustion systems, where the fuel is injected early on in the compression stroke at a low pressure and is ignited with the use of a spark plug. The NO_x emissions can be reduced by adopting measures such as lean-combustion and exhaust gas recirculation [13]. Hydrogen combustion engines require carefully balanced thermodynamic parameters such as the injection technique, air-fuel mixture, valve timing, and ignition timing to realize stable and efficient engine operation [4].

Despite these challenges, hydrogen combustion offers cost benefits compared to other carbon-neutral means of propulsion - by using the already widespread process chain of conventional combustion engines [13], as research on hydrogen in-

ternal combustion engines is significantly shaped by traditional internal combustion engines given that the combustion model is essential for both. Retrofitting conventional four-stroke diesel and petrol engines for hydrogen fuel requires minimal modifications to manufacturing processes when compared to completely new power-train technologies. This adaptability allows OEMs to re-purpose existing engine designs while meeting emissions regulations through relatively simple modifications.

When designing an engine of this kind, engineers utilize and iterate through tools such as 3D Computational Fluid Dynamics (CFD), 0D/1D modelling, and single-cylinder engine (SCE) testing to develop the appropriate combustion systems. This thesis focuses on the use of 0D/1D simulation tools and SCE testing and how they can be used to realize a full-scale multi-cylinder engine (MCE) concept.

0D/1D simulation methods are a valuable early-stage combustion development tool and are used to provide fast and efficient modeling of complex systems by simplifying their physical representation. In engine development, 0D/1D simulations are used to analyze overall system behavior—such as pressure, temperature, and flow rates—across components like cylinders, manifolds, and pipes, without resolving detailed spatial variations. This method is valuable for system-level analysis and early-stage design. It enables engineers to quickly evaluate performance, optimize control strategies, guide designs, and allows for more informed 3D simulations of combustion systems and flow components. However, standalone models require the fuel burn to be imposed onto the model - which is a challenging task for pre-mixed hydrogen combustion.

The single-cylinder engine is used as a tool to physically prototype and test engine systems. It includes a decoupled testbed configuration that can help to accelerate our understanding and optimize a combustion system before moving to a full-scale engine. A proposed combustion system, once designed with CFD and 0D/1D simulation methods, can be validated in an SCE test bench. Isolating one cylinder enables conducting detailed studies on fuel injection, ignition timing, combustion efficiency, and new technologies without the complexity and cost of a full multi-cylinder engine.

This thesis work relies on the integration of experimental data obtained from a pre-mixed hydrogen SCE into a Hardware-in-Loop (HIL) test environment. A particular focus is placed on the acquisition of in-cylinder pressure traces, which are analyzed using a special simulation tool called a three-pressure analysis (TPA) model. This model computes the apparent burn rate of the fuel combusted in the

SCE. These burn rates are imposed on a 0D/1D MCE simulation model, enabling a more realistic representation of the combustion behavior of a pre-mixed hydrogen MCE at system level.

The output of the MCE provides a set of boundary conditions that can be related to the physical SCE and used to adjust actuator settings of the test bench at the inlet and exhaust manifolds - achieving steady state convergence between the physical SCE and the MCE model in these boundaries is of interest, allowing us to represent the combustion of an MCE system within a controlled SCE environment.

In addition to building up an experimental modeling framework, the thesis will investigate methods for efficient data exchange between the SCE test bench and simulation platforms. It will assess the sensitivity of the system to cycle-to-cycle variations and updates to the boundary conditions which are a challenge in hydrogen combustion.

A core ambition of this project is to demonstrate how a data-driven, near real-time modeling approach can significantly reduce development time and cost in the field of hydrogen engine research.

1.2 Aim

This project work evaluates whether data from single-cylinder experimental testing can enhance the accuracy of 0D/1D multi-cylinder concept models. By bridging the gap between physical testing and virtual simulation, the study seeks to accelerate development timelines and improve the design quality of next-generation engine concepts.

1.3 Research Questions

The central focus of this study is to investigate whether calculating the burn rate from the pressure trace of a physical SCE provides a significant advantage for engine concept development. This section breaksdown the research questions investigated. Specifically, the research explores whether using experimental results to calculate boundary conditions and burn rates for a simulated MCE yields better results than relying exclusively on a stand-alone MCE simulation with a predictive combustion model imposed on the system.

- **In the context of premixed hydrogen combustion, does calculating the burn rate from the pressure trace of a physical SCE, then using it to calculate boundary conditions for a simulated MCE model, offer an advantage for engine concept development compared to relying on a standalone MCE simulation**

The overarching research question is a complex and demanding research task. Resource and time limitations during the course of the project hindered the full solution to the proposed problem. Instead, the foundation of this project was laid, which aims to aid in the continuation of its work. This was done by breaking down the research question above into research questions 1.1 and 1.2, which are then further evaluated in the results section of this paper.

1.1. Sensitivity to Cyclic Variations:

- **How sensitive is the burn rate and boundary condition in the simulation due to cyclic variations of premixed hydrogen spark-ignited data input?**

This analysis examines how sensitive the burn rate and simulated boundary conditions are to the cyclic variations inherent in experimental input data from premixed hydrogen spark-ignited tests. The objectives of the study were to assess the sensitivity of the simulation's boundary conditions to the input data and to determine an optimal input data size. The end goal of the study was to determine the minimum input data size while maintaining sufficient resolution and accuracy in the simulation output.

1.2. Correlation and Accuracy:

- **How accurately does a system-level 1D MCE model, simulated using burn rates from experimental SCE tests and three pressure**

analysis, correlate with experimental MCE combustion data?
This objective assesses the accuracy of a system-level 0D/1D MCE model. It evaluates how closely the simulation (driven by burn rates calculated from a TPA model and experimental SCE test data) correlates with actual experimental MCE combustion data from an engine with similar geometry and operating conditions.

2

Theory

2.1 Pre-mixed Hydrogen Combustion

Hydrogen can serve as a primary energy carrier and can be produced from renewable sources like wind, solar, and biomass. Unlike carbon-based fossil fuels, which are a major contributor to CO_2 emissions, burning pure hydrogen ideally produces only water as a byproduct [10]. Hydrogen combustion offers a lower cost of transition because hydrogen internal combustion engines (H2ICEs) can utilize existing infrastructure developed for gasoline and diesel based engines [14].

Combustion processes are classified into diffusion and pre-mix combustion, based on whether the fuel and oxidizer are mixed before or during the combustion reaction. Diffusion combustion occurs when the reactants are not mixed beforehand and must mix in the same region where the combustion reaction takes place. In premixed combustion, the fuel and oxidizer are well mixed before spark onset [6].For internal combustion engines, this is usually done with Port Fuel Injection (PFI) or Direct Injection (DI).

Premixed hydrogen combustion offers a viable pathway for high-efficiency, carbon-free energy generation. Hydrogen's unique physical properties set its premixed combustion apart from hydrocarbons. It has a wide flammability range in air, from 4% to 75% by volume, which enables ultra-lean combustion, where engines can use much more air than needed for a stoichiometric mixture [14]. This allows for unthrottled operations at low to medium loads, eliminating pumping losses associated with the pressure drop across the throttle plates [18]. Ultra-lean combustion can also reduce peak temperatures and significantly lower nitrogen oxide (NOx) emissions [10]. Hydrogen has a high laminar flame speed, about 1.85 m/s in a stoichiometric mixture, which is enabled through the fuel's quick reaction rate and large diffusion coefficient [10]. This enables rapid heat release and high thermal efficiency. When compared to hydrocarbon-air mixtures, hydrogen combustion has a significantly lower minimum ignition energy [14]. Hydrogen needs less than one-tenth the energy required to ignite petrol at the same air-fuel ra-

tio (AFR). Because of the short ignition delay and high autoignition temperature ($\tilde{8}$58K), pre-mixed hydrogen combustion is mainly used in spark ignition (SI) engines. Due to these characteristics, hydrogen combustion is highly sensitive to operational parameters. The unique physicochemical properties of hydrogen necessitate advanced fuel handling systems and precise electronic control strategies. While it enables high power density, insufficient control can lead to combustion instabilities, which pose significant risks to hardware integrity, efficiency, and operational safety[9] [17] [19].

2.2 Cyclic Variations

Cyclic variations are a phenomenon in SI engines when the combustion process varies from cycle to cycle. The main causes of cyclic variations are in the early combustion phase, especially in the formation of the flame kernel after the spark discharge. These variations are caused by: fluctuation in gas movement at ignition, variations in the air-fuel ratio, non-homogeneous air-fuel mixing and internal EGR[6].

These changes are observed as fluctuations in the cylinder pressure, which can lead to incomplete combustion and, in the worst case, misfire. The consequence of this is reduced fuel efficiency and engine performance. In hydrogen engines, it is especially important to control these variations[1]. Depending on the air-fuel ratio, the combustion stability of premixed hydrogen is relatively high, with the Coefficient of Variation (CoV) of Indicated Mean Effective Pressure (IMEP) ($\mathrm{CoV_{IMEP}}$) remaining less than 1% at medium and high loads in certain cases. However, as the air-fuel mixture becomes more lean, it becomes more prone to cyclic variations and misfires, limiting the practical extent of lean operation [4]. Abnormal combustion events are still one of the toughest problems for premixed hydrogen engines. Studies show that reducing cycle variability can increase power output by up to 10% without increasing fuel consumption [3]. Cyclic variations have a direct impact on how a vehicle drives and feels, especially when the engine runs in lean-burn conditions [14].

2.3 Single Cylinder Engine Testing

2.3.1 Purpose

The SCE test bed is a build configuration that typically includes an isolated combustion system from a MCE. It is widely used in the development phase of an engine or combustion system. It offers a number of benefits which range from direct validation of a combustion system component to fuel testing and research. Practically, the benefits of using a SCE test bed include:

- **Reduced Complexity:** The SCE build simplifies the testing environment. Instrumentation is focused on a stand alone combustion environment, reducing the density of sensors and supporting hardware otherwise required on an MCE testbed. Furthermore, the control logic is reduced; whereas an MCE requires complex coordination of multiple injectors and thermal management systems, an SCE scales these requirements down to a single unit.
- **Accelerated Development Cycle:** Managing design iterations is more efficient with an SCE. The simplified assembly allows engineers to iterate between designs quickly, reducing the downtime associated with engine rebuilds in MCE configurations.
- **Economic Advantage:** SCE testing is significantly more cost effective due to a lower component count. In MCE testing, a single design change may necessitate a complete engine overhaul. The modular nature of an SCE allows for more frequent and economical hardware iterations.

Considering these practicalities, SCE testing has an important place in powertrain Research and Development (R&D). The need for testing in an SCE is driven by several factors listed as follows [6] [11].

- **Design Evaluation and Validation:** Allowing for the evaluation of a prototype combustion system. This allows engineers to fine tune the operation settings which define its use case and ultimately strives to validate a combustion systems design.
- **Safety and Product Liability:** Engineers are able to expose the combustion system to abnormal combustion, designing to prevent the phenomena and mitigate the inherent negative consequences.
- **Measuring Improvements:** Allows for a means to track improvements and evolve a prototype combustion system.
- **Statistical Data Collection:** Statistical data is collected for fine tuning, reliability analysis, and performance rating.

The goal of the engineering team is to disassemble each of these components into their foundational development criteria. In context of the above factors the engineering team uses the SCE to collect data for optimizing performance, efficiency,

emissions, structural integrity, individual component selection/design, and reliability and durability evaluation

2.3.2 Data Typically Collected

In this project the SCE is a critical component in ensuring the successful development of the "Virtual MCE" design tool. The data acquisition system (DAQ) embedded into the SCE system is used to recorded crank angle resolved and time averaged data. In general crank angle resolved data includes values sampled from the following locations:

- Raw pressure signal from within the combustion chamber.
- Inlet manifold pressure
- Exhaust manifold pressure
- Spark plug ignition current
- Injector rail pressure and injector needle valve control current
- Calculated parameters calculated in real time from the collected data:
  - Apparent heat release (Also includes a normalized value)
  - Apparent heat release rate
  - Knocking parameter calculation

Time-averaged parameters are monitored to characterize the engine's performance. These measurements typically, among other parameters, encompass Exhaust After-Treatment System (EATS) chemical species, regional temperature sampling, turbocharger settings and feedback, and EGR ratios. Collecting data at this temporal resolution allows for a macro-scale evaluation of the system's thermodynamic, mechanical and chemical equilibrium.

2.3.3 Testing methodologies Overview

Experimental evaluation using a SCE is a targeted process primarily focused on the characterization and optimization of a combustion system's operational parameters. For a low pressure direct injection (LPDI) system (such as that in this research), the SCE provides a controlled environment to establish the performance across a predefined range of engine speeds and loads.

To map the engine's performance, a Design of Experiments (DoE) approach is employed. This methodology is executed in phases aimed at decoupling complex variables and identifying the sensitivities of the combustion. Testing is performed at discrete steady-state setpoints, defined by engine speed and IMEP according to ISO standard 15550:2016 [6][8].

The experimental process generally consists of parametric sweeps where individual variables are iterated while maintaining constant boundary conditions. Key control parameters include:

- **Energizing (Fuel Injection):** Start of Energizing (SOE), End of Energizing (EOE), and rail pressure.
- **Ignition and Valve Timing:** Spark timing based on a desired CA50, which is often set at 8 CAD after top dead center.
- **Gas Exchange:** EGR rates and AFR - provides data for the development/selection of effective boosting systems and their control.

Following parametric sweeps, a comprehensive optimization of the engine's operation is conducted. This phase aims to synthesize the data collected from the parametric sweep into a coherent calibration strategy. Some primary outputs of the optimization include the following parameters.

- **Efficiency Metrics:** Indicated Brake Thermal Efficiency and Brake Specific Fuel Consumption (BSFC).
- **Emission Profiles:** Specifically NOx concentrations.
- **Combustion Stability:** Usually quantified by CoV_{IMEP} and knock parameters.

3

0D/1D Simulation and GT-Suite Setup

3.1 Overview with a Hydrogen Combustion Perspective

Modeling and simulation play an increasingly important role in developing premixed hydrogen combustion engines. Researchers use advanced 3D-CFD to analyze mixture formation and flame propagation, which supports improvements in combustion chamber design. Because detailed chemistry in 3D-CFD simulations is resource intensive, initial studies are often conducted in a 0D/1D environment using tools such as GT-Suite [4].

0D/1D engine simulations are physics based tools that model how fluids move, heat is transferred, and chemical reactions occur in an ICE. These tools use basic conservation equations for mass, momentum, and energy. The engine's flow systems are represented as a network of 1D pipes and ducts, while the cylinders are treated as 0D spaces where pressure and temperature can change over time but remain even at any moment [5]. This method allows engineers study key engine features like power, torque, volumetric efficiency, and fuel use without spending much time or money on physical prototypes [12]. For hydrogen engines, 0D/1D modeling is especially helpful for early research on high laminar flame speed and wide flammability range, which require careful system-level control.

Modeling hydrogen combustion in a 0D/1D environment is challenging because these approaches assume the cylinder contents are evenly mixed, which ignores the spatial differences and shapes that lead to cyclic variations. This is important because hydrogen combustion reacts strongly to hot spots and how well the gases mix. Since these simple models cannot capture the real physics behind these variations, 0D/1D modeling needs a lot of experimental data and careful calibration to make up for this [15].

3.2 Two-Zone Combustion Methodology

GT-Power uses a two-zone combustion methodology to simulate the combustion process for nearly all engine models except for Homogeneous Charge Compression Ignition (HCCI) models and certain predictive diesel models. This is the standard approach for predicting in-cylinder pressure and temperature, as it accounts for distinct thermodynamic states of the gases in zones. This is the method used during the course of this research. The two zone models detailed as according to the Gamma Technologies Engine Performance Manual. [5].

3.2.1 Core Mechanism

The two-zone methodology operates in the following manner:

- At the start of combustion, the cylinder volume is divided into two homogenized thermodynamic zones: an unburned zone and a burned zone. Initially, all cylinder contents, including the fresh air-fuel mixture, residual gases from the previous cycle, and any EGR gases, are placed in the unburned zone.
- As the simulation progresses, a portion of the air-fuel mixture is transferred from the unburned zone to the burned zone at each timestep. This transfer rate is defined by the burn rate, which represents the instantaneous fuel consumption. The burn rate can either be imposed (non-predictive) or calculated (predictive) by the combustion model.
- Once the unburned mass is transferred to the burned zone in a given timestep, GT-Power performs a chemical equilibrium calculation for the entire burned zone. The calculation identifies all the atoms of each species present in the burned zone, and from this, it takes into account the equilibrium concentration of the standard combustion products. The resulting species concentration is strongly dependent on the instantaneous temperature and pressure in the burned zone.
- After the new composition is determined in the burned zone, the internal energy of each species is summed to find the total energy of the burned zone. GT then applies the principle of energy conservation to solve for the new temperatures in both zones and the resulting cylinder pressure.

3.2.2 Governing Equations

The two-zone combustion model solves two primary energy equations in each time step. For the unburned zone, the equation is:

$$\frac{d\left(m_u e_u\right)}{dt} = -\,p\,\frac{dV_u}{dt} - Q_u - \left(\frac{dm_{f,b}}{dt}\,h_f + \frac{dm_{a,b}}{dt}\,h_a\right) + \frac{dm_{f,i}}{dt}\,h_{f,i} \tag{3.1}$$

where:

m_u : unburned zone mass
$m_{f,b}$: fuel mass transferred to burned zone
$m_{a,b}$: air mass transferred to burned zone
$m_{f,i}$: injected fuel mass
e_u : unburned zone energy
p : cylinder pressure
V_u : unburned zone volume
h_f : enthalpy of fuel mass
h_a : enthalpy of air mass
$h_{f,i}$: enthalpy of injected fuel mass
Q_u : unburned zone heat transfer rate

And for the burned zone, the equation is:

$$\frac{d\left(m_u e_b\right)}{dt} = -\,p\,\frac{dV_b}{dt} - Q_b + \left(\frac{dm_{f,b}}{dt}\,h_f + \frac{dm_{a,b}}{dt}\,h_a\right) \tag{3.2}$$

where:

m_b : burned zone mass
$m_{f,b}$: fuel mass transferred to burned zone
$m_{a,b}$: air mass transferred to burned zone
e_b : burned zone energy
p : cylinder pressure
V_b : burned zone volume
h_f : enthalpy of fuel mass
h_a : enthalpy of air mass
Q_b : burned zone heat transfer rate

3.3 Three-Pressure-Analysis Model

Three Pressure Analysis (TPA) is a modeling method in GT-Suite that calculates the apparent burn rate of an engine cylinder using measured pressure data. The model uses a reverse run calculation, further described in Section 3.3.1, in a two-zone combustion setup. TPA predicts all trapped quantities in the cylinder by

simulating flow through the valves. The method uses three inputs: intake, cylinder, and exhaust pressures. By using the intake and exhaust pressures as boundary conditions, the model predicts the gas exchange process. This allows the model calculate the residual gas fraction and trapping ratio of the cylinder and is seen as a more accurate way to determine the burn rate from measured pressure data, especially at part-load conditions [5].
Two types of analysis can be done using the TPA:

- **TPA steady**: The simulation analyzes measurement data for deriving a single combustion burn rate. The input pressure data is either averaged or limited to a single cycle.
- **TPA multicycle**: This method requires instantaneous pressure data over multiple cycles as input.

Since a goal of this thesis is to obtain system-level boundary conditions and system-level stability using a derived burn rate, this study focused on the TPA steady method.

3.3.1 Reverse Run Calculation

GT-Power uses a special logic called a reverse run calculation. It uses the measured cylinder pressure from a test environment as input to calculate the apparent burn rate. In the standard forward run calculation, the burn rate is the input, and pressure is the calculated output. The reverse run uses the same governing equations, thermodynamic principles, and two-zone combustion methodology as in the forward run. This ensures that the calculation follows the full chemical and thermodynamic laws applied in a forward run without any simplified assumptions.

In a reverse run calculation, the amount of mass transferred from the unburned zone to the burned zone is iterated at each timestep until the calculated pressure matches the measured cylinder pressure input at that timestep. This allows us to reproduce the cylinder burn rate from the test environment in the simulation. GT-Power has two methods for calculating the apparent burn rate using the reverse run methodology [5].

- Closed Volume Analysis
- Three Pressure Analysis

This thesis focused on the TPA methodology.

3.3.2 Required Data Input

The TPA model requires primarily three pressure measurements from the cylinder of interest: intake port pressure, exhaust port pressure, and cylinder pressure.

These measurements must be crank angle resolved. The data required for successful simulation includes:

- **Dynamic Pressures:** Crank angle resolved instantaneous intake, exhaust, and cylinder pressures.
- **Time-Averaged Temperatures:** Measured average temperature at the same locations as the pressure sensors for intake and exhaust.
- **EGR data:** Average air mass flow rate and EGR flow rate.
- **Fuel injection data:** Injected fuel mass, timing and timing.
- **Spark Timing:** For Spark Ignition(SI) engines
- **Drive Shaft Load:** Standard engine dynamometer data for model setup
- **Geometric Data:** For the engine cylinder, valves, and ports are required to build the model.

3.3.3 Model Setup

A TPA normally has a single-cylinder engine layout. The model comprises ports, runners (if present), valves, the cylinder, and the Engine crank train component built following standard modeling procedures. Modelling components in this section are referred to according to the GT Engine Performance Manual.

A significant feature of the TPA setup is the implementation of port pressures as boundary conditions using the BoundaryPressureTPA template. This template uses a special logic to vary the temperature around the measured average in response to the pressure fluctuations and reverse flow. It also manages the thermodynamic mass composition during both forward and reverse flow to ensure that the fluid properties entering and leaving the cylinder are accurately represented. For engines with external EGR this template allows specifying the EGR fraction directly, which is then used to mix fresh charge with the exhaust products from the cylinder.

In the cylinder template, an EngBurnRate reference object must be used for TPA steady, and the Cylinder Pressure Analysis Mode should be set to "Analysis, Full Cycle (TPA)".

To reduce numerical noise and prevent pressure signal fluctuations, the model requires specific pipe discretization and time-stepping settings. The discretization length for the intake and exhaust ports should be lowered to around 20% of the cylinder bore for intake ports and 25% for exhaust ports. The maximum time step in the flow control of the run setup must be limited to 0.25 degrees. These changes are required because the BoundaryPressureTPA template attempts to match the input pressure data in the first sub-volume of the attached pipe, and too large

sub-volumes or time steps might generate unnatural feedback fluctuations.

Static pressure boundaries can cause pressure fluctuations within the ports when the valves are closed. To ensure that the predicted pressure behavior is consistent with the measured data, a control system is required to damp these reflections. This is done by using the friction multiplier in the pipe sub-volume directly adjacent to the BoundaryPressureTPA template. When the valve is closed, the multiplier is increased to a large value (around 100) to damp the reflections. When valves are open, the value goes back to being 0 for ports or 1 for runners.

If the TPA is adapted from a pre-existing full engine model, the injector templates need to be replaced with an InjPulseConn template, which maintains the injection profile. An inaccurate port injection profile can alter the resulting pressure waves. Another factor to consider while setting up the TPA model is the timing of the simulation cycle. The start of cycle attribute in EngineCrankTrain must be set to a value that occurs after IVC but before the start of the combustion event.

3.3.4 Simulation Methodology

The TPA model follows the same governing equations and two-zone combustion methodology used in the standard forward run simulations. During the simulation, GT-Power follows a special iterative sequence:

- For the first cycle, a dummy burn rate is used, and no pressure analysis is performed.
- For the second cycle, the forward run simulation will pause at the start of the cycle and will calculate the apparent burn rate by iterating the mass transferred between the combustion zones until the predicted pressure matches the input measured pressure at each timestep. The injection profile and heat transfer data will be carried over from the previous cycle. Once the entire burn rate profile is calculated, the forward simulation run continues.
- This process is iterated from cycle two and beyond until steady state convergence is reached.

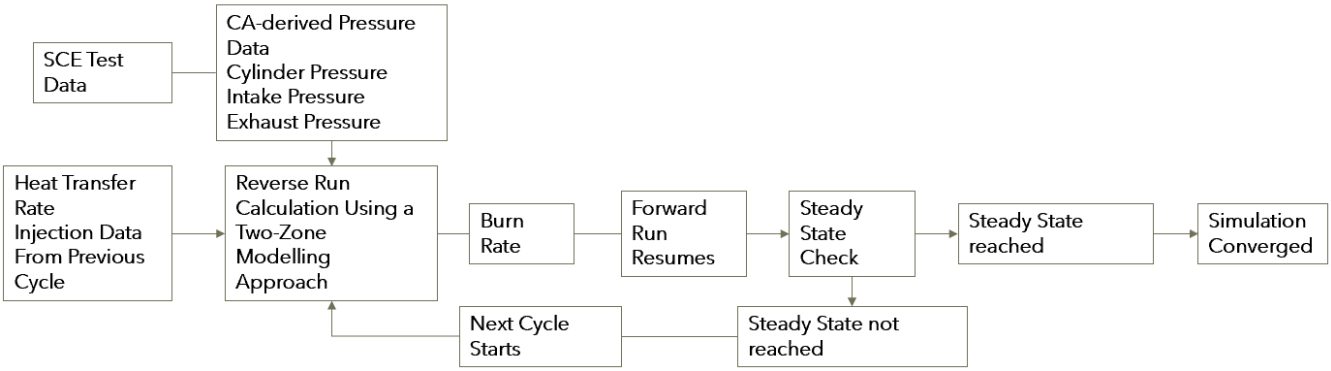

Figure 3.1: Flow chart of TPA simulation methodology

3.3.5 Consistency Checks

GT-Power runs consistency checks to validate the integrity of the model setup and measured data [5].

Deriving the burn rate from measured cylinder pressure involves some errors caused by pressure transducers, sensors, modeling assumptions, and simplified thermodynamics. These combine to a cumulative error, which will almost never be zero. As a result, the total available fuel mass in the cylinder will not match the predicted fuel burned during the simulation. GT-Suite then adjusts the fuel energy to achieve a combustion efficiency or burned fuel fraction derived from input test data using an LHV multiplier. If the required LHV adjustment goes above 5%, it is flagged as an error.

The integrated IMEP based on the cylinder pressure must be compared to the measured BMEP. If the resulting IMEP is not greater than the BMEP by a value proportional to the engine's FMEP, it implies errors in the measured data.

For steady-state analysis, the measured pressure profile input is shifted to ensure the best match at the start of the cycle. A shift of more than 0.5 bar will be flagged as an error. When the cylinder is being compressed before the start of combustion, the integrated fuel burned should be close to zero. If the cumulative burn during this period goes above 2% of the entire fuel, it is flagged.

In direct injection models, GT checks if there is sufficient fuel in the cylinder to meet the expected burn rate. It is flagged as an error if the missing fuel goes above 2%. For steady state runs using input measure data, GT-Power compares the simulated air mass at IVC, fuel mass, and air-fuel ratio against the measured

data. If the deviations are above 5%, it is flagged as an error.

Even a 1 degree crank angle phasing error will have an impact on the integrated IMEP. It can be identified by examining a motoring pressure trace, which should peak around 0.5-1.5 degree before TDC (set the encoder error at 0.7 CAD BTDC as a rule of thumb). Errors in the absolute pressure might shift the entire profile. It is visible as curvature after IVC and inconsistencies during the pumping loop. Deviations in the designed compression ratio can show up in the LogP-LogV at the end of the compression stroke, as a low compression ratio in an upward curvature and a high compression ratio in a downward curvature.

3.3.6 Result Evaluation and Export

Once converged, the results are stored in a .glx file. Plot groups are generated for comparisons between the measured and simulated pressures, apparent burn rate, etc. For TPA steady runs, an EngCylCombProfile object is created, which can be imposed in subsequent forward run models to reproduce the experimental test rig combustion behavior. This allows the TPA modeling methodology to function as a bridge between physical testing and predictive simulation calibration.

3.4 MCE Modeling

A MCE model is built from three main parts: EngCylinder objects for each combustion chamber, an EngCrankTrain that sets up the mechanical link and firing order, and a set of valves, pipes, and manifold connections for gas exchange. The EngCylinder and EngCrankTrain form the main structure for referencing key physical processes like combustion, heat transfer, and friction. Each cylinder connects directly to the EngineCrankTrain, and GT gives each one a global cylinder number based on its port connection. This number is important because it sets the engine's firing order. Cylinders connect to the intake or exhaust manifolds using valve connection templates, which define how the cylinder valves flow. These valves link the cylinders to the ports, which are modeled with pipes and flow splits to represent the size and heat transfer features of the cylinder head [5].

The fluid dynamics of the intake and exhaust manifolds have a significant impact on the performance of a MCE. GT models these systems using one-dimensional fluid dynamics, solving the Navier-Stokes equations to represent flow and heat transfer within the piping network. This allows for representing the pulsating flows and wave dynamics that are necessary for estimating volumetric efficiency, power, and torque with different operating speeds.

For MCE models with three or more valves per cylinder, the model must have additional valves and ports connected by flowsplits. To accurately represent the pressure losses due to contraction or expansion, the expansion diameter of the flowsplit connecting to the manifold must match the physical diameter in the cylinder head. For accurate gas exchange predictions, the model needs well-resolved valve discharge coefficients. This is important in the MCE models with EGR because the backflow of exhaust gases into the intake manifold during the valve overlap period can affect the trapped residual fraction and subsequent combustion simulation.

MCE models use two modes in the EngCrankTrain: speed mode and load mode. *Speed mode* is for steady state simulations where we set the engine speed, and the solver finds the matching brake torque. This mode is efficient because it skips the time needed for the crankshaft to reach steady speed under load. *Load mode* is for transient studies where a load is applied, and the solver calculates engine speed using brake torque, load torque, and system inertia. During transient simulations in load mode, the rotating inertia of the engine and accessories is important for predicting speed changes accurately. In these simulations, we can set operating conditions like turbocharger waste gate positions and AFR with lookup maps or predictive controllers. This lets the model react to changing loads, which is important for drivability and fuel economy analysis [5].

A full MCE model needs to include sub-models such as turbochargers, charge air coolers, and EGR circuits. Turbochargers act as feedback systems, and their performance can be represented with turbine and compressor maps. Some cases might require the need for mass as well as efficiency multipliers to match experimental results from engines running under pulsating conditions[5].

An EngCylCombProfile template may be used to directly impose a burn rate on the model. This is an ideal approach to implement a non-predictive model (TPA). To increase calculation efficiency, GT has a Cylinder Copying feature, which allows the solver to execute detailed calculations on a single cylinder and reproduce the results in the other cylinders. This reduces the CPU time required while maintaining a reasonable accuracy for the steady state. In real-time or long transient simulations, a detailed engine model can be converted into a Fast Running Model (FRM) or by using Mean Valve Engine Modeling. These methods can considerably reduce the simulation time required to run an MCE system [5].

4

Methodology and Experimental Setup

4.1 Virtual MCE Data Exchange and Loop Development

This chapter characterizes the interface developed to bridge the gap between experimental engine testing and simulated environments. By decomposing the system into its constituent hardware and software elements, the text explains the operational workflow and the optimization of component parameters. The section concludes with an analysis of the control logic and the programming architecture that facilitates real-time data exchange.

4.1.1 Overview

A Python-based communication protocol was developed to orchestrate data exchange between the experimental SCE, the TPA and MCE models, and the test rig data acquisition (DAQ) systems and control systems. This integrated environment, referred to as 'The Loop', manages the overall feedback to the system controller and the internal feed-forward data streams essential for system operation. Figure 4.1 provides a schematic overview of the backend data exchange architecture in its intended closed loop implementation.

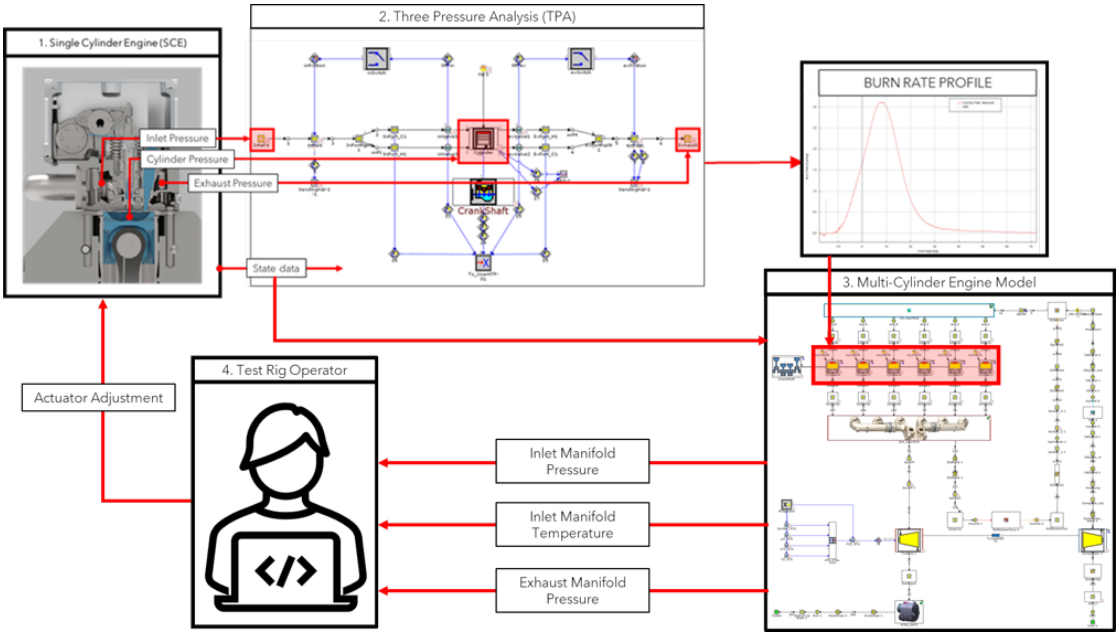

Figure 4.1: Virtual MCE data exchange loop required for the realization of the "virtual MCE"

Figure 4.1 illustrates the synchronization of time-averaged state data and crank-angle resolved pressure data acquired from the SCE (1), described in section 4.1.3, and shows its integration into the TPA model (2), described in section 4.1.5. The TPA model calculates the apparent burn rate profile - referred to simply as the 'burn rate' - and is then imposed as a combustion condition across all cylinders of the MCE model (3), which is further detailed in section 4.1.6. To achieve loop convergence, the MCE simulation yields critical thermodynamic outputs, specifically the intake manifold temperature (T_{in}), manifold pressure (P_{in}), and exhaust back pressure (P_{exh}). These parameters are transmitted to the test rig operator, who adjusts the physical SCE environment to reflect the simulated boundary conditions. This iterative process continues in closed loop until a set of steady state convergence criteria, detailed in Section 4.1.8, are satisfied.

The converged Loop yields output performance metrics, and complex gas dynamics and thermodynamics for a simplified 0D/1D environment at a burn rate which is true for its operational conditions with system level fidelity. The output of this MCE model was then compared with experimental results extracted from a MCE (further detailed in Section 4.1.2), which served as the catalyst for the development of the MCE simulation model.

4.1.2 Multi-Cylinder Engine

An experimental engine was used for validation of the simulated MCE. The reference project was a developed 13-liter, six-cylinder inline spark-ignition (SI) engine specifically engineered for hydrogen combustion. To manage boost pressure and transient response, the engine utilized a Variable Geometry Turbocharger (VGT) regulated via a PID control loop. Furthermore, the system incorporated an Exhaust Gas Recirculation (EGR) circuit to optimize combustion stability and emissions. A rendering of the engine is presented in Figure 4.2. The engine was part of a project titled "HYCET" at Volvo, and was tested at the KST engine test labs in Germany. For this reason the name HYCET and KST MCE are used interchangeably in the text and figures of this thesis.

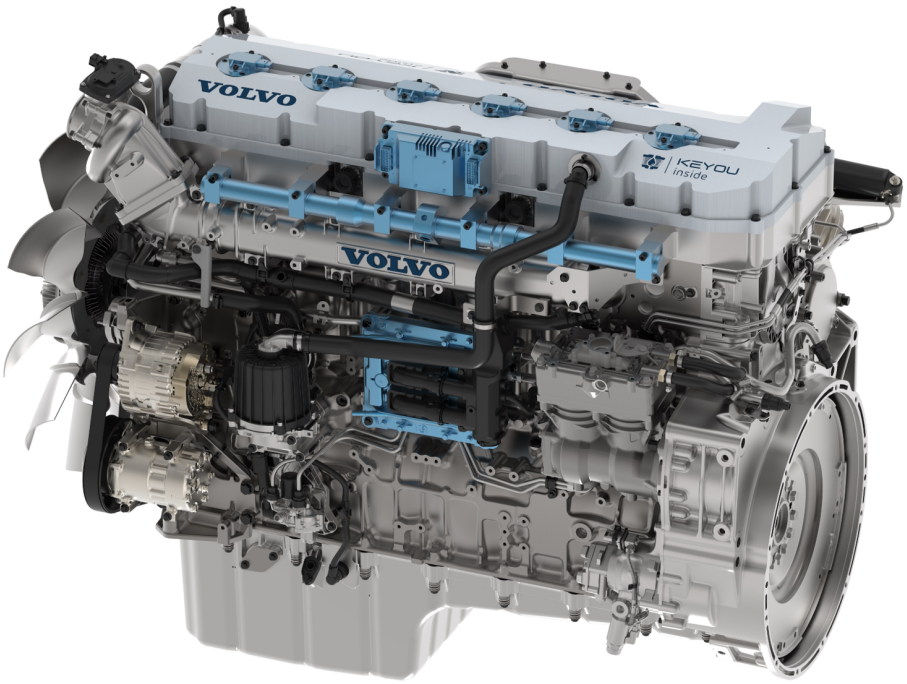

Figure 4.2: Render of the HYCET engine

The geometry of some key combustion system components are detail below.

Variable	Description	Value
V	Total volume	13 L
r_c	Compression ratio	9.7
B	Bore	131 mm
L	Stroke	157 mm
l	Conn. rod length	259 mm

Table 4.1: HYCET/KST MCE geometric properties

4.1.3 KIT Single Cylinder Engine

The experimental phase of this research was conducted using data from a SCE at Karlsruhe Institute of Technology (KIT). Utilized by Volvo for advanced powertrain development, the KIT SCE was selected for its architectural commonality with the HYCET MCE project. A render of the KIT SCE is provided in Figure 4.3, with its specific geometric parameters detailed in Table 4.2.

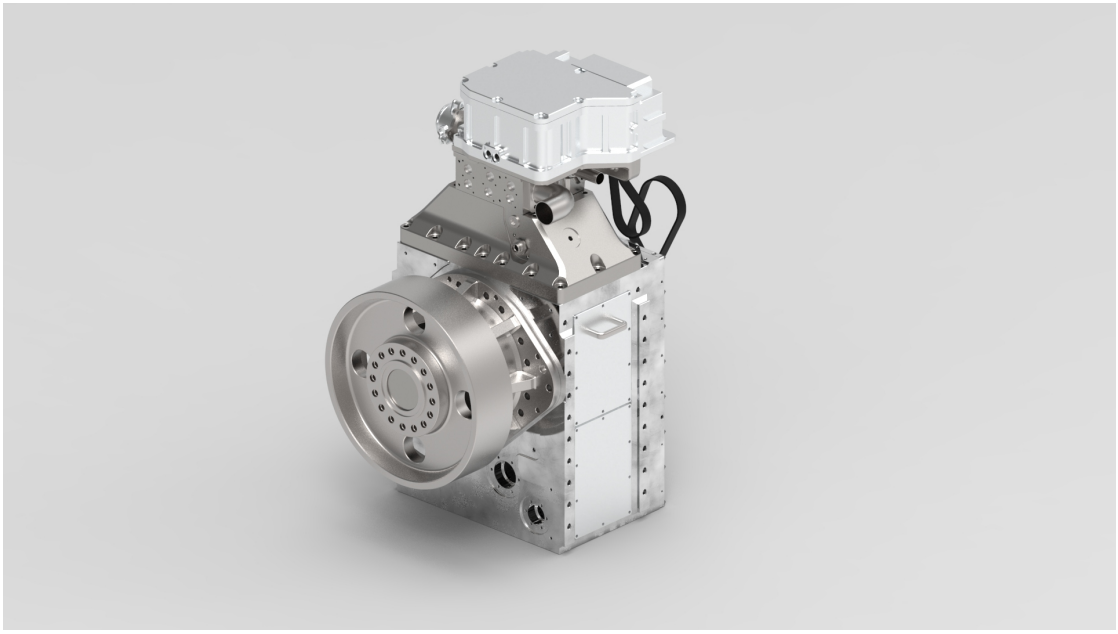

Figure 4.3: Render of the KIT single cylinder research engine.

Variable	Description	Value
V	Total volume	2.12 dm^3
r_c	Compression ratio	9.7
B	Bore	131 mm
L	Stroke	157 mm
l	Conn. rod length	277 mm

Table 4.2: KIT SCE geometric properties

4.1.4 KIT SCE and MCE comparison

A standard bowl-shaped piston served as the basis for development between the engines. KIT utilized a Bosch Injector and designed the cylinder head to accommodate a lateral injector placement and a central spark plug. The lateral injector

enabled fuel-tumble mixing to be realized - aligning with the mixing methodology used in the HYCET engine. The fundamental arrangement of the injector and spark plug resembled one another sufficiently to be deemed interchangeable for this study. The MCE utilized an injector from Hoerbiger and possessed minor discrepancies in the injector and spark plug angles. Figure 4.4 shows the specific details of this difference.

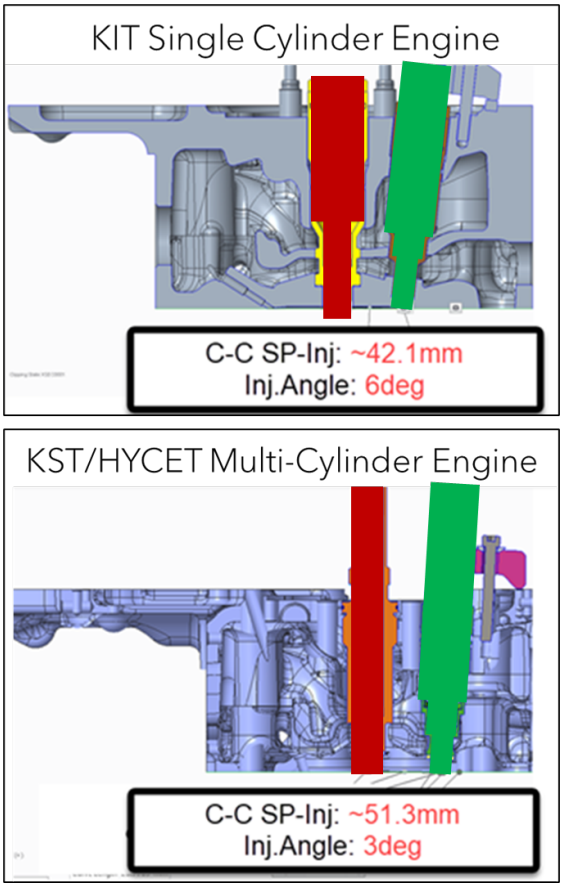

Figure 4.4: Comparison of the injector and spark plug angles between the KIT test bench and the KST/HYCET test bench.

Furthermore, in Table 4.1 and Table 4.2 it should be noted that the connecting rod lengths do not match one another. A study was conducted to investigate this effect and referring to Figures B.1 and B.2 in the appendix it was found that no significant change existed.

It is important to note that the HYCET specifications are the baseline from which the KIT configuration was built - allowing the KIT SCE to serve as a detailed

follow-up platform for results obtained from the HYCET MCE. However, since the development of these test setups, experimentation and development was conducted independently. Subsequently, this independence introduced a series of limitations on the quality of available data, which is further detailed in section 7.1.2.

4.1.5 Three-Pressure Analysis Model

A TPA model was configured based on the geometry of the KIT SCE. Figure 4.5 below shows a screenshot of the TPA model developed for this project. From a cross section of the SCE the general location of the piezoelectric pressure transducers are shown with arrows denoting the simulation components where these CA resolved pressure traces are imposed.

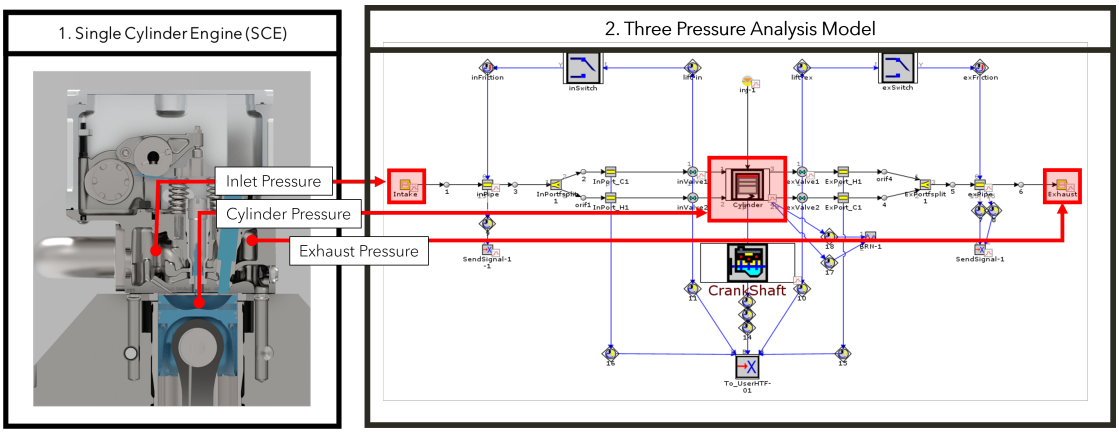

Figure 4.5: Three Pressure Analysis model and corresponding data sources

4.1.5.1 Gas Exchange

The gas exchange system within the TPA model comprises the following functional elements:

1. Intake runner (inlet pipe)
2. Intake port bifurcations (intake pipe split)
3. Dual intake and exhaust valve assemblies
4. Combustion system control volume (Acting as a pumping device)
5. Exhaust port junction (merging flow from exhaust valves)
6. Exhaust runner (outlet pipe)

High fidelity was maintained by ensuring that the geometric dimensions, specifically diameters, lengths, and volumes, precisely replicate the physical architecture of the KIT SCE. In alignment with Gamma Technologies (GT) modeling conventions, the geometry is abstracted into a one-dimensional (1D) framework. Within

this environment, discrete frictional and pressure losses in the piping are not modeled explicitly; instead, these losses are consolidated into discharge coefficients (C_d) specific to the cylinder head, piston, and valve geometry, as per the GT engine performance manual [5]. Furthermore, the cam arrays for the inlet and exhaust valves were explicitly defined in accordance with those that were installed on the KIT SCE.

4.1.5.2 Combustion System

The combustion system is parameterized within the crankshaft and cylinder modules, as illustrated in Figure 4.5. These computational objects facilitate the definition of the engine's reciprocating assembly and combustion chamber architecture, including the piston crown (bowl) geometry, cylinder liner dimensions, and connecting rod length. Furthermore, the firing order and the thermophysical properties of the constituent materials are specified to replicate the KIT SCE configuration. Detailed parameter values are tabulated in Table 4.2.

4.1.5.3 Injectors

Fuel injection parameters were implemented using a simplified r square wave step function approach. Although complex needle-lift dynamics and spray-wall interactions are present and their affects can be modeled using rail pressure and injector current profiles, this study utilizes a constant mass flow rate to represent the injection event. The duration is governed by the start of energizing (SOE) and end of energizing (EOE) setpoints, resulting in a step-function injection profile. This abstraction ensures that the total fuel mass delivered per cycle remains consistent with experimental data while simplifying the boundary conditions for the TPA and MCE models.

It should be noted that this assumption does not affect the net energy content of the model but does affect the heat transfer modeling, which considers the effects of turbulence and squish in the combustion gases. The effect of this assumption was considered to be minor in the scope of the research; however is a topic put forward as a recommendation for further development.

4.1.6 Multi-Cylinder Engine Simulation

The simulation platform for this research is a 0D/1D GT-Suite model based on the MCE developed during the HYCET project. The initial architecture, comprising of the gas exchange system, turbocharger, EGR loop, and core engine geometry, was constructed by Volvo engineers prior to this study for the HYCET project's

development. Consequently, the model is assumed to be a high-fidelity representation of the engine's physical geometry. To adapt this MCE framework for The Loop's application, specific geometric refinements were implemented. These modifications included minor adjustments to the inlet and exhaust valve diameters, updating the connecting rod length, and redefining the cam profiles to match the SCE hardware. The final model layout is illustrated in Figure 4.6.

Instead this geometry was maintained from the original model supplied by Volvo.

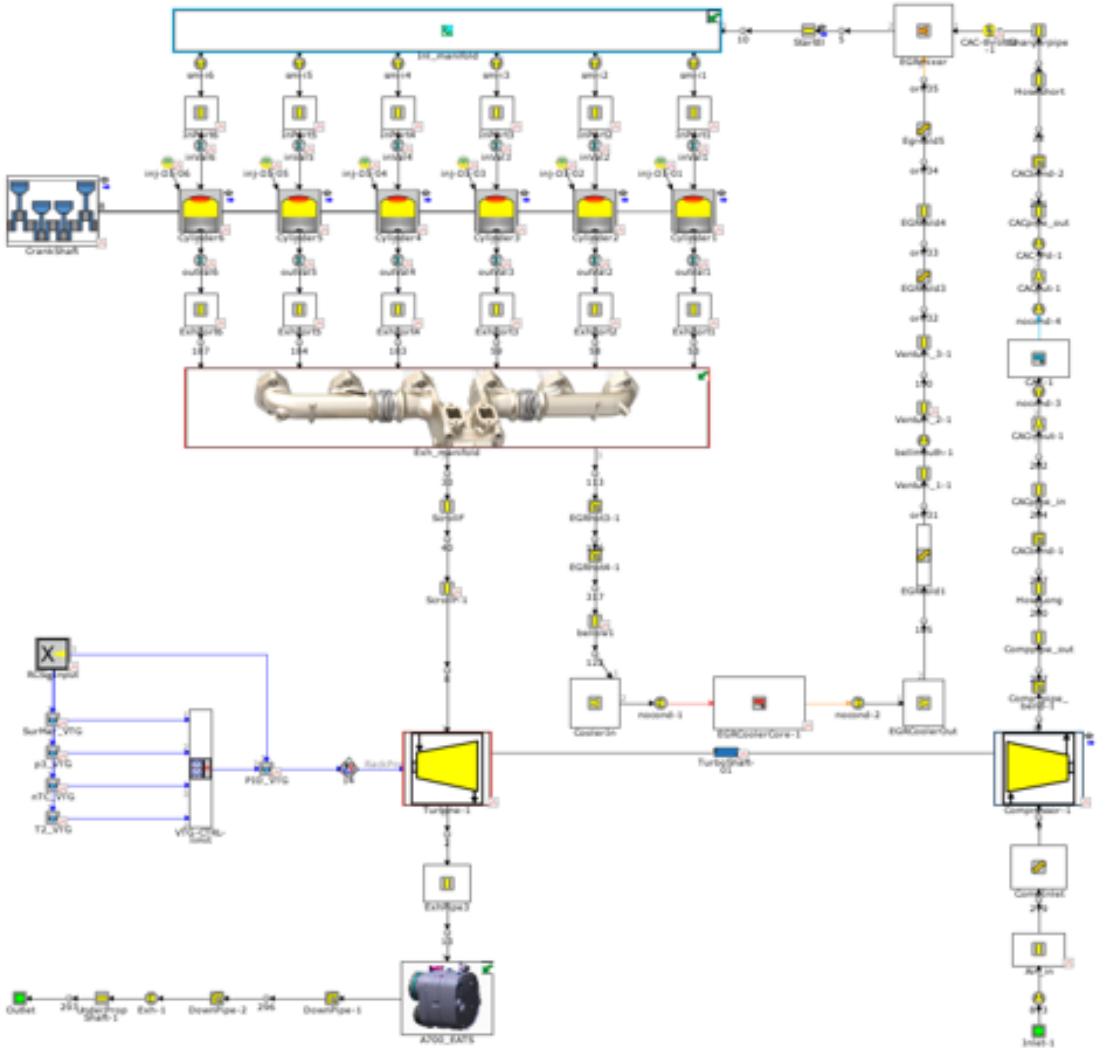

Figure 4.6: 0D/1D GT-Suite model of the HYCET multi-cylinder engine

The combustion system geometry of the MCE is define in table 4.3 below:

Variable	Description	SCE Value	MCE Value
V	Total volume	2.12 L	13 L
N_{cyl}	Number of cylinders	1	6
r_c	Compression ratio	9.7	9.7
B	Bore	131mm	131 mm
L	Stroke	157 mm	157 mm
l	Conn. rod length	277 mm	277 mm
$D_{invalve}$	Inlet valve diameter	42 mm	42 mm
$D_{exhvalve}$	Exhaust Valve Diameter	40 mm	40 mm

Table 4.3: MCE geometric properties

4.1.7 Data Exchange

4.1.7.1 Simulation Setup

To facilitate near real-time synchronization between the experimental test rig and the simulation environments, an automated data-polling function was developed. Upon the deposition of a new experimental dataset into a designated directory on the Volvo servers, the integration program automatically detects the update and initiates the processing workflow.

The acquired data is categorized into two distinct streams based on sampling frequency. The first, termed 'slow data,' comprises time-averaged parameters sampled at regular intervals. These are initially captured in raw *.mdf* and *.mdp* formats before being processed by the Volvo Data Science Lab (DSL) into high-performance *.parquet* files. Slow data typically includes thermodynamic state variables, mass flow rates, and fluid temperatures.

Conversely, high-frequency data, referred to as fast data, consists of crank-angle resolved measurements. This data includes current measurements, pressure data and several parameters relating to the heat release calculation. Of interest was the intake manifold pressure (P_{in}), in-cylinder pressure (P_{cyl}), and exhaust manifold pressure (P_{exh}), with sampling locations indicated in the SCE, shown in Figure 4.1. Initially recorded as raw *.ifile* files, these raw files are directly utilized by the TPA upon upload to the Volvo servers. These files are also subsequently converted to *.parquet* format via the DSL pipeline, providing further options for post-processing.

The developed software extracts simulation-critical parameters from both high-frequency (fast) and low-frequency (slow) raw datasets to ensure the TPA and MCE models accurately reflect the physical experimental environment. A Mi-

crosoft Excel-based interface serves as the centralized data exchange hub between the processed experimental outputs and the simulation environments. By utilizing the GT-Suite Data Link functionality, the simulation objects are automatically updated based on the values populated in this Excel interface. A simplified representation of this configuration template is illustrated in Figure 4.7. This standardized format not only streamlined the parameterization process but also provided a transparent framework for benchmarking SCE experimental results against simulated outputs.

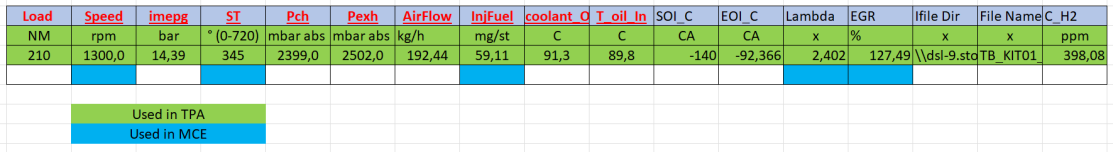

Load	Speed	imepg	ST	Pch	Pexh	AirFlow	InjFuel	coolant_O	T_oil_In	SOI_C	EOI_C	Lambda	EGR	Ifile Dir	File Name	C_H2
NM	rpm	bar	° (0-720)	mbar abs	mbar abs	kg/h	mg/st	C	C	CA	CA	x	%	x	x	ppm
210	1300,0	14,39	345	2399,0	2502,0	192,44	59,11	91,3	89,8	-140	-92,366	2,402	127,49	\\dsl-9.sto	TB_KIT01_	398,08

Used in TPA
Used in MCE

Figure 4.7: Excel file used to setup the simulation environments of the TPA and MCE models. The use of parameters are color coordinated for the simulation model.

4.1.7.2 Burn Rate Profile

The apparent burn rate profile is the output of the TPA model and is stored as a 2D numerical array which includes the crank angle degree (CAD) sampled every 0.1 CAD and the corresponding fuel mass per CAD during the engine cycle.

This burn rate profile is stored as a *.trn* file. The GT-Suite MCE model is then configured to read this file from its directory and imposed it into each cylinder in the MCE model.

4.1.7.3 Boundary Conditions

After imposing the burn rates from the TPA model the MCE will then solve for the flow, heat transfer, momentum and energy balance. Once these have reached steady state convergence the output will be the boundary conditions of the MCE that are required to realize the imposed SCE combustion. This can be visualized with figure 4.8. As mentioned previously the parameters of interest are P_{in}, P_{exh} and T_{in}. A reporting function is used within the developed software to facilitate the extraction of these boundary conditions and the creation of a file to store these values. These values are then passed by the loop application to the test rig operator (or control system) according to figure 4.1.

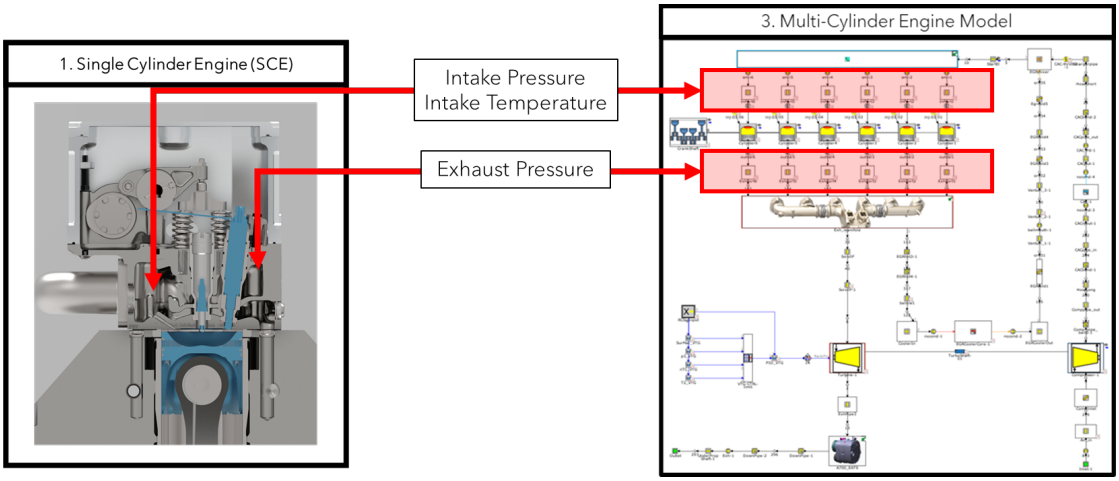

Figure 4.8: Data exchange between the SCE and virtual MCE which governs steady state closed loop convergence

4.1.8 Loop Convergence

Convergence is defined as the state in which the variation in boundary conditions between successive loop iterations remains within the prescribed tolerance window specified in Table 4.4. This steady-state equilibrium is contingent upon the operating point being physically and computationally attainable by both the SCE and MCE platforms. To ensure empirical validity, the convergence thresholds are derived from the measurement uncertainty and resolution limits of the integrated sensor hardware, ensuring that the loop terminates only when further iterations fall below the level of acceptable change.

Parameter	Accuracy	Tolerance
P_{in}	±0.05 kPa	±2 kPa
T_{in}	±1C	±5C
P_{exh}	±0.05 kPa	±2

Table 4.4: Convergence tolerance of boundary condition parameters on the MCE to the SCE

4.1.9 Multi-Cylinder Variation and Reference Selection

The MCE simulation treats the engine as a holistic system; consequently, the gas exchange dynamics are explicitly modeled, resulting in non-uniform performance across individual cylinders. This variation is anticipated in both the experimental

and simulated MCE environments due to the inherent complexities of manifold wave dynamics and mass flow distribution.

The variance in performance is illustrated in Figure 4.9, which displays the average work performed by each cylinder in the experimental engine. For the purposes of this study, results from Cylinder 5 (both virtual and experimental) are utilized for comparison to ensure consistency. Cylinder 5 was selected because it represents the median work output recorded during experimental testing, serving as a statistically representative baseline for the comparative analysis of the wider iterative loop. This load point was also checked for knock and sensor errors - cylinder 5 passed both knock and error checks and more can be read about this in Appendix C

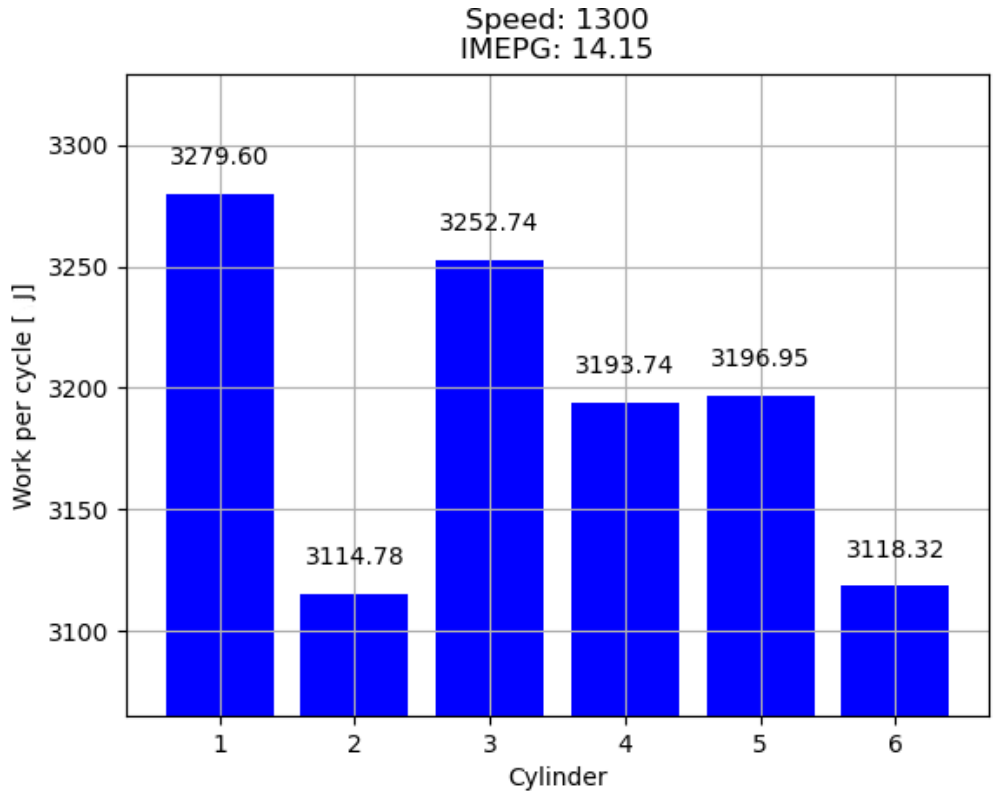

Figure 4.9: Average indicated work done by each cylinder

4.2 Research Question 1.1: How sensitive is the loop to Cyclic Variations

This study examined how the loop's boundary conditions respond to the pressure data entered. The pressure data covers the crank angle resolved instantaneous intake, exhaust, and cylinder pressure, which are used to calculate the burn rate in the TPA model. The research looked at how using different sizes of cycle average data, as well as cycles with median and max IMEP, affects the results. Data from 10 raw data files (**.ifiles**) were used for this study. Samples 9 and 10 are also used to address research question 1.2.

Sample No.	**IMEP (bar)**	**CoV (%)**	**Lambda**	**Speed (rpm)**
Sample 1	11,15	4,3	2,801	1100,1
Sample 2	14,01	3,9	2,547	1100,1
Sample 3	11,15	2,8	2,813	1100,1
Sample 4	11,01	4,0	2,786	1100,1
Sample 5	11,09	3,8	3,071	1100,1
Sample 6	9,47	3,2	3,111	1100,1
Sample 7	7,85	4,3	3,073	1100,1
Sample 8	7,82	3,9	3,060	1100,1
Sample 9	14,40	4,1	2,402	1300,0
Sample 10	14,39	4,1	2,427	1300,0

Table 4.5: IFile sample data operating points

In the TPA steady method, GT-Power averages all input pressure data into a single average cycle for analysis. For this study, custom cycle data were extracted from the .ifiles and averaged using a Python script with the CATool package. Cycle data of various sizes was extracted and used as input to the loop, ranging from 0-5 cycles to 0-200 cycles, along with cycles with the median and max IMEP. A 200-cycle average was taken as the standard input for each sample. Results were extracted from GT-POST, compiled, and subsequently plotted using Excel. The analysis of the TPA and MCE model simulation results focused on the following parameters:

Category	Parameter
Indicated Performance	$IMEP_{net}$ (IMEP720 – Net Indicated Mean Effective Pressure) $IMEP_{gross}$ (IMEP360 – Gross Indicated Mean Effective Pressure) Indicated Efficiency Combustion Efficiency Volumetric Efficiency (Air)
Combustion Phasing & Duration	Crank Angle at 10% Burned (CA10) Crank Angle at 50% Burned (CA50) Burn Duration 0–10% Burn Duration 10–90%
Energy & Losses	Cumulative Energy Loss
Pressures	Maximum Cylinder Pressure Intake Cylinder Pressure Exhaust Cylinder Pressure
Temperatures	Intake Temperature Exhaust Temperature

Table 4.6: Combined list of MCE combustion, performance, and gas-exchange parameters

4.3 Research Question 1.2: How well does the simulated MCE compare to experimental MCE data

As mentioned in Section 4.1.2 and 4.1.3, the KIT SCE was derived from the HYCET project's multi-cylinder architecture to facilitate a direct comparative analysis. By adapting a standard bowl-shaped cylinder head to include a central spark plug and lateral injector, the KIT SCE replicates the fuel-tumble mixing strategy employed by the HYCET/KST Multi-Cylinder Engine (MCE). While minor geometric variations in injector-plug orientation exist, the shared piston geometry and injector specifications render the SCE a high-fidelity platform for following up on MCE results. However, the their independent development of these

platforms introduces specific data limitations, which are addressed in Section 7.1.

Section 5.3 aimed to show how the results from the simulated MCE represented the experimental results from the HYCET engine. The research question was answered by analyzing the full engine cycle with a LogP-LogV diagram and discusses the difference that were observed with particular focus on the cylinder pressure, pumping loop and inlet manifold pressures. Analysis was also conducted into differences observed in the volumetric efficiencies and the indicated efficiencies. The limitation of the study are discussed in section 7.1.

5
Results

5.1 Loop Output and Performance

5.1.1 Inlet Manifold Convergence

Inlet temperature and pressure are governing parameters for convergence, directly impacting the calculated burn rate. Consequently, these values dictate the boundary conditions and overall performance output of the MCE simulation. The iterative process aims to constrain these variables within the predefined limits established in Table 4.4.

As illustrated in Figure 5.1, the manifold pressure exceeds the permissible threshold during the initial iteration, necessitating further computational cycles. At this specific load point, the KIT and MCE exhibit a relative pressure deviation of 6.7% after the first iteration. According to the convergence criteria, the allowable error is defined as a function of boost pressure, where increased boost levels dictate a more stringent error margin. Consequently, a maximum relative absolute error of 0.8% — equivalent to a differential of ± 2 kPa between the MCE and SCE — is required to satisfy the convergence targets. It should be noted that this level of convergence accuracy should be tested and validated. In the absence of a means to validate these convergence limits on a dedicated research engine, it is unknown if these limit are obtainable or if greater tolerances are possible. As a result, it is put forward as a recommendation to test these convergence parameters for future development on dedicated hardware.

In Figure 5.2, a thermal discrepancy exists between the measured SCE and simulated MCE. To satisfy the imposed burn rate profile, a target inlet temperature of 49.2 C was identified for the MCE. Consequently, further iterative loops are necessary to achieve numerical convergence. Consistency between the experimental data and the TPA results further validate the TPA model, exhibiting a relative error of only 0.7%.

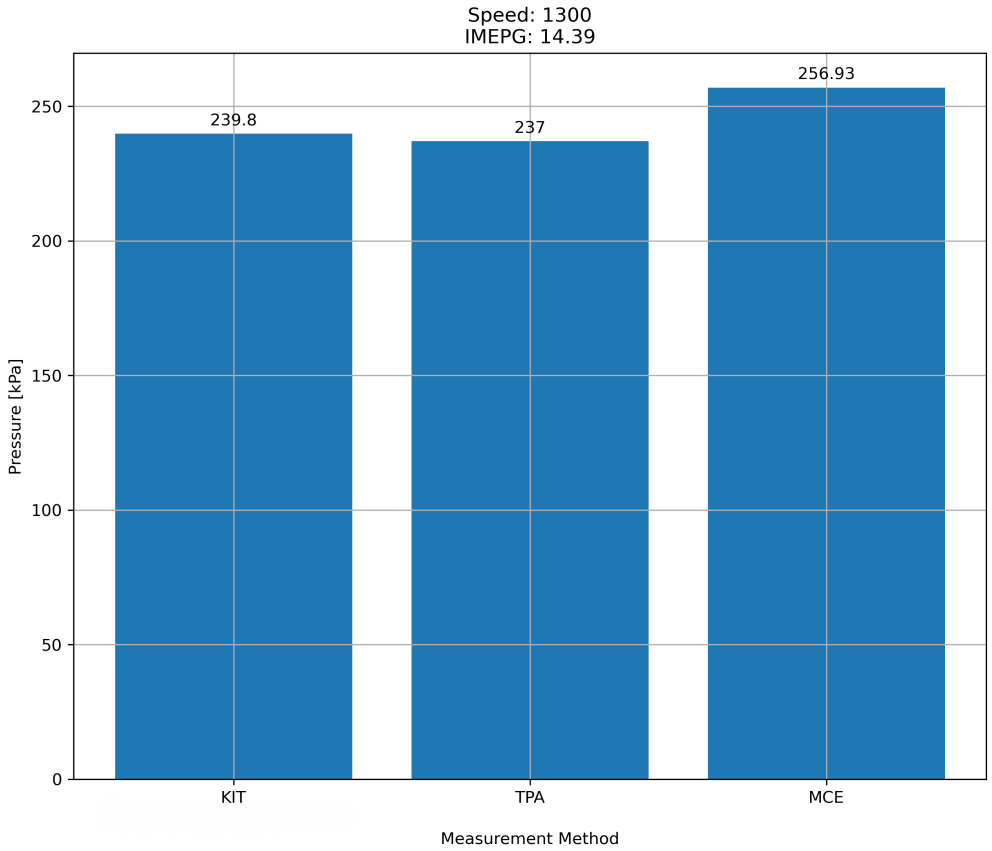

Figure 5.1: Inlet manifold pressure

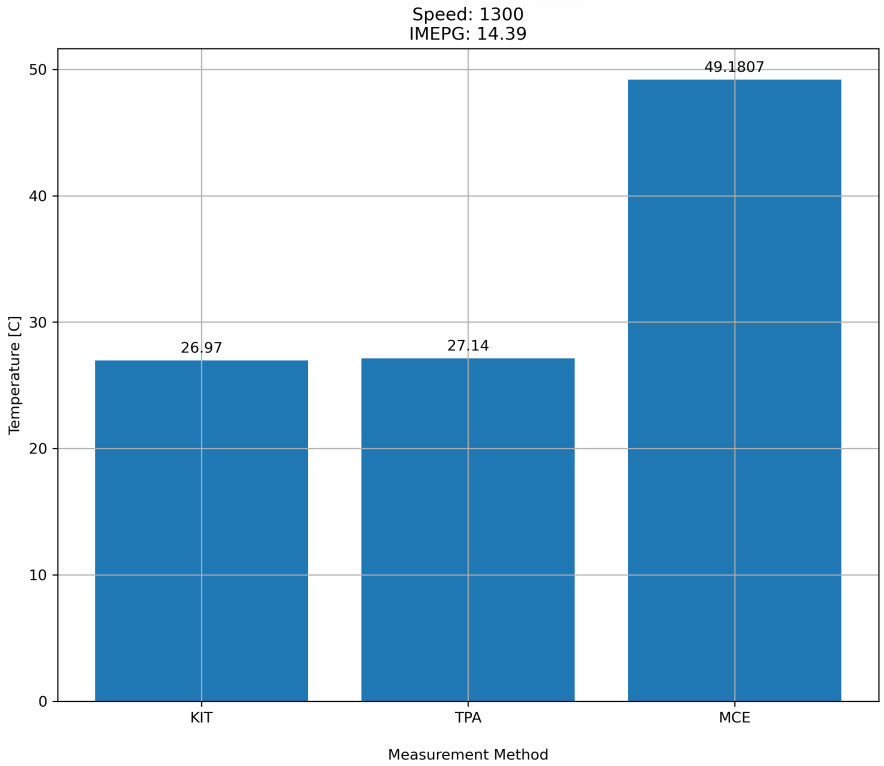

Figure 5.2: Inlet manifold temperature

5.1.2 Exhaust Manifold Convergence

Regarding the analysis of the exhaust data extracted from the virtual MCE, it should be noted that data was collected at two distinct locations within the exhaust system. The first location, indicated by the orange bar in Figure 5.4 and 5.3, corresponds to the exhaust port exit immediately downstream of the cylinder. The second location, indicated by the green bar, is situated at one of the two 3-to-1 collectors (serving cylinders 1-3 and 4-6, respectively).

Defining these spatial differences is of critical importance as gas wave dynamics vary significantly between these two sections; however, both are relevant to this study. Port-level measurements capture the discrete, high-amplitude pulse dynamics of a single cylinder once per four-stroke cycle, allowing for the characterization of localized heat transfer effects.

In contrast, the manifold measurement is subjected to the combined flow of all three cylinders connected to the single collector. In this case, the individual gas pulses are superimposed out of phase according to the engine's firing order and valve timings. This interference results in a time-averaged mean gas temperature and pressure recorded across three cylinders, which increased the effective temperature measurement and decreased the measured pressure. The impact of this phenomenon was found to be more significant for temperature, and was comparatively less pronounced for the pressure measurements.

With regards to exhaust boundary pressure, the exhaust readings for the SCE and MCE had smaller relative errors than what was observed in the inlet manifold. A relative error of 3.8% was measured. The explicit values fell outside of the convergence requirements defined in table 4.4.

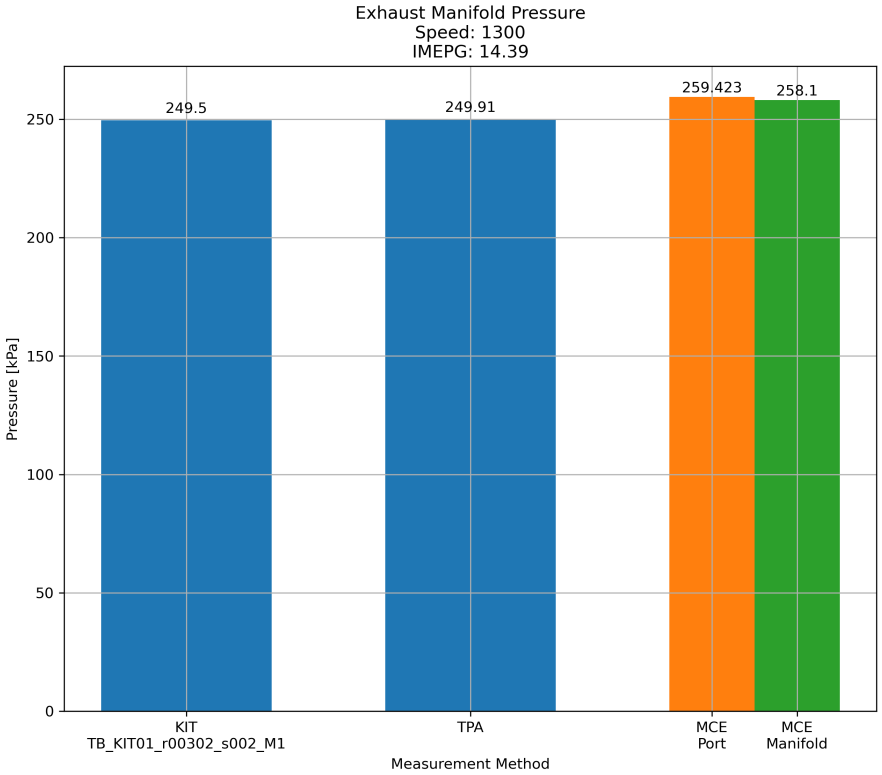

Figure 5.3: Exhaust manifold pressure

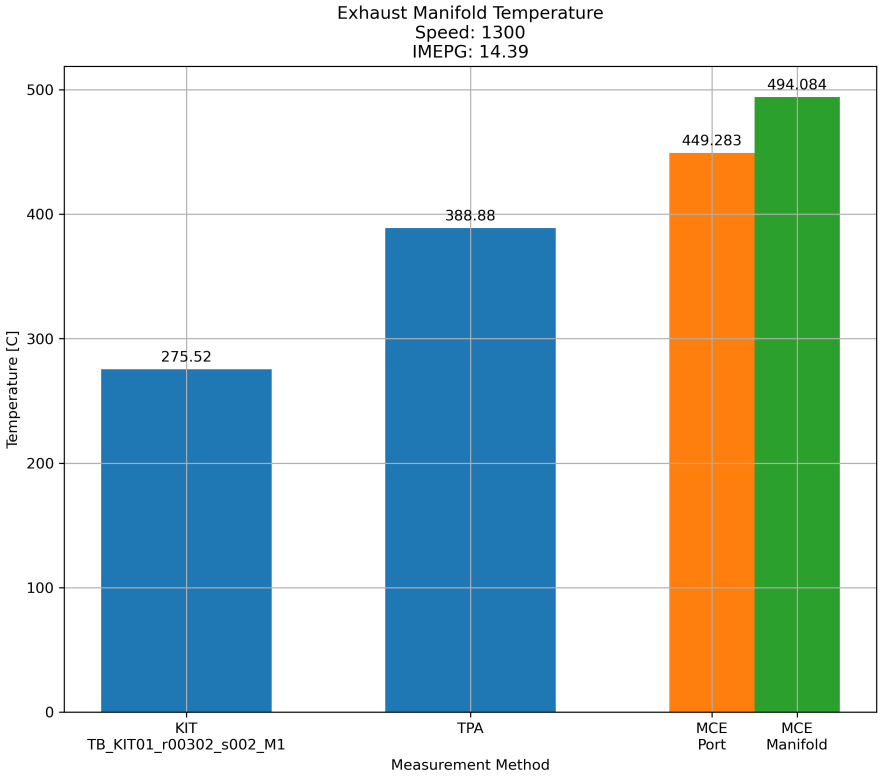

Figure 5.4: Exhaust manifold temperature

5.1.3 Operational Efficiency

Figure 5.5 shows the time taken by each process independently. The simulations were the largest bottle neck with each submission to a simulation cluster taking approximately 3 minutes regardless of the whether the simulation was submitted to a high performance cluster or if it was simulated on a local computer. Amounting to a total of 6 minutes dedicated to simulation. In addition to this, approximately 2 minutes is required to adjust the boundary condition with a further minimum 2 minutes dedicated to data collection from the SCE and operations to impose this data.

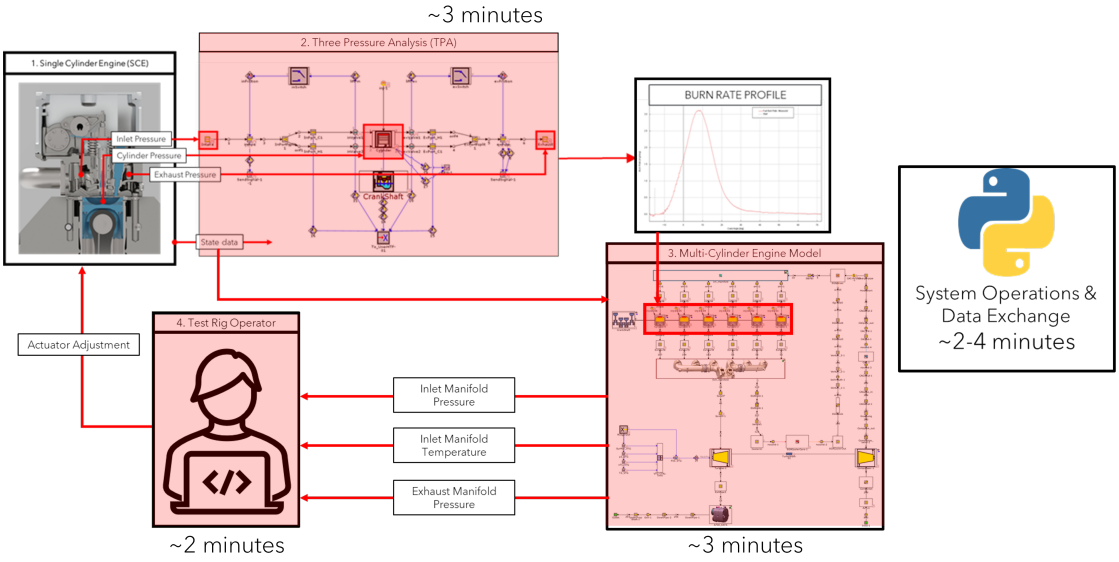

Figure 5.5: Processing time evaluation.

The expected time to conduct a single Loop iteration is estimated at 10 minutes. It should be further investigated if the benefits of developing this virtual MCE outweigh this temporal disadvantage. This should consider the fact that this method has the potential to greatly increase the maturity of an MCE concept before a physical prototype is required - which is a timely and costly process in itself. The engineer should also bear in mind that this system would be required to go through the full range of engine tests to realize a high fidelity output of the final MCE product (assuming that R&D is conducted on the MCE continuously). More about this can be read in Section 2.3.

5.2 Research Question 1.1: How sensitive is The Loop to Cyclic Variations

The following section discusses the findings related to research question 1.1. When observing how the loop responds to changes in the pressure trace input, using different sample sizes to average the pressure traces of the same sample file in the loop gave very similar boundary results in the MCE model.

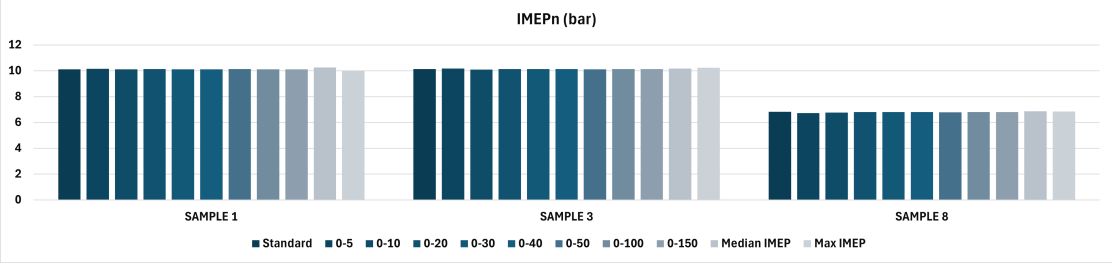

Figure 5.6: IMEP output from the loop

When the IMEP output using a standard input of 200 pressure trace cycles was compared, the largest change in output IMEP from the loop was less than 3.5%. Plots with all the sample size data have been added to the appendix for reference.

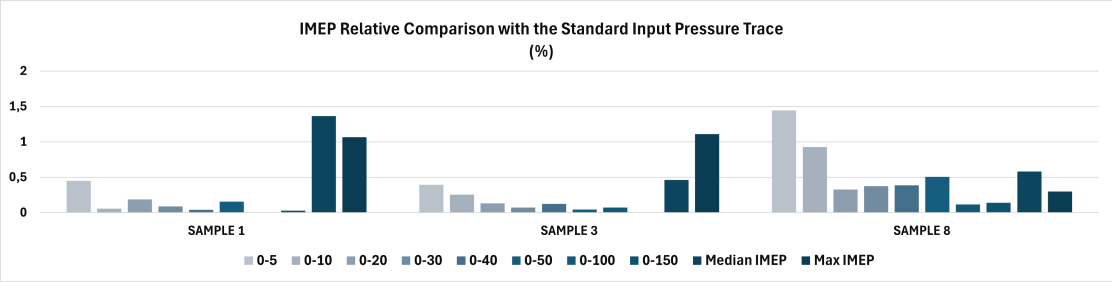

Figure 5.7: IMEP Relative Comparison with the Standard Input Pressure Trace

The results were consistent for other observed indicated output performance parameters from the loop. The biggest change in the indicated performance parameters came from using a single pressure cycle with either the median or maximum IMEP. In contrast, using the averaged cycle as input resulted in a relative change of less than 1.5% compared to the standard input.

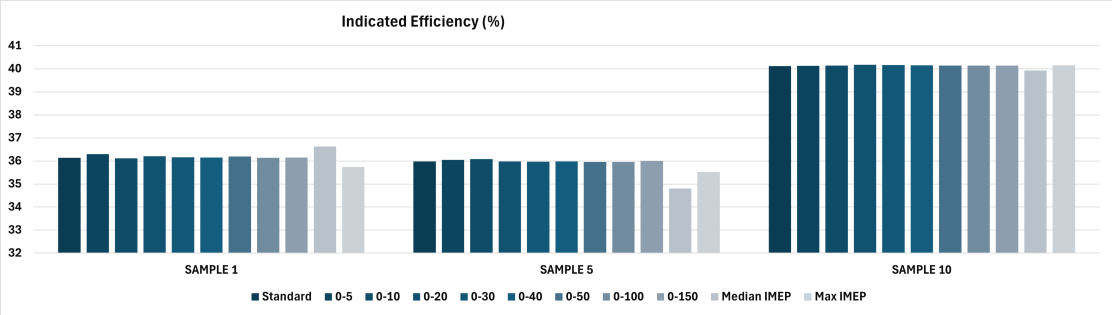

Figure 5.8: Indicated Efficiency output from the loop

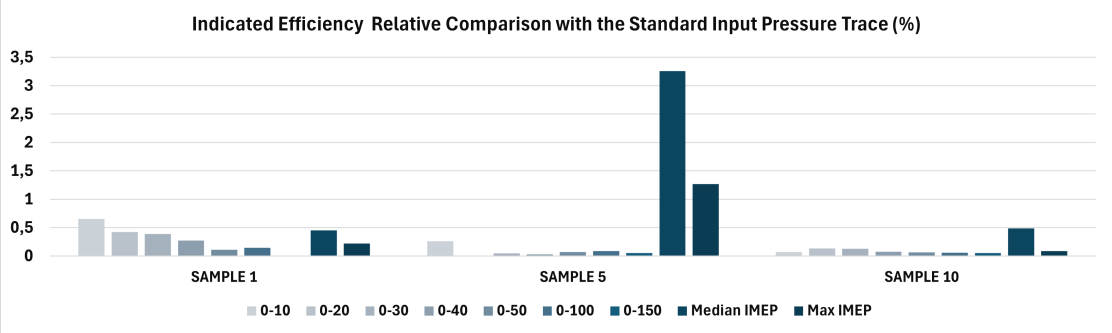

Figure 5.9: Indicated Efficiency Relative Comparison with the Standard Input Pressure Trace

An analysis of the sensitivity of boundary pressure conditions to the input pressure trace showed minimal changes in boundary pressure outputs compared to the standard input, consistent with the indicated performance results.

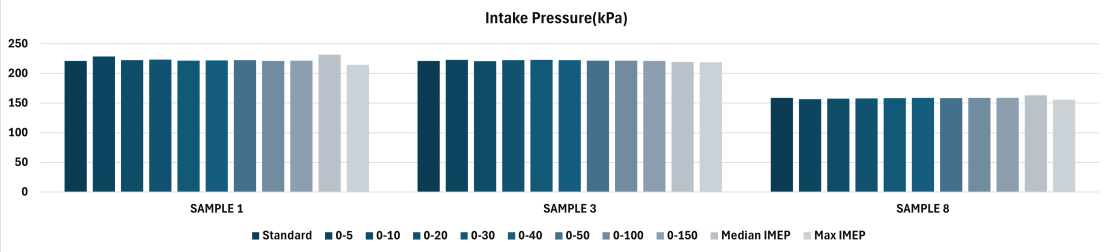

Figure 5.10: Intake Pressure output from the loop

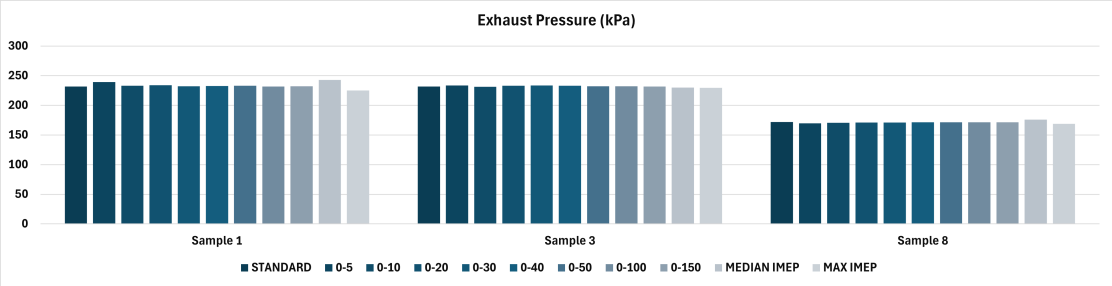

Figure 5.11: Exhaust Pressure output from the loop

The largest relative change was observed when using a single pressure trace with median or maximum IMEP. In contrast, averaging the cycle input over 10 or more cycles reduced the relative change to less than 2%.

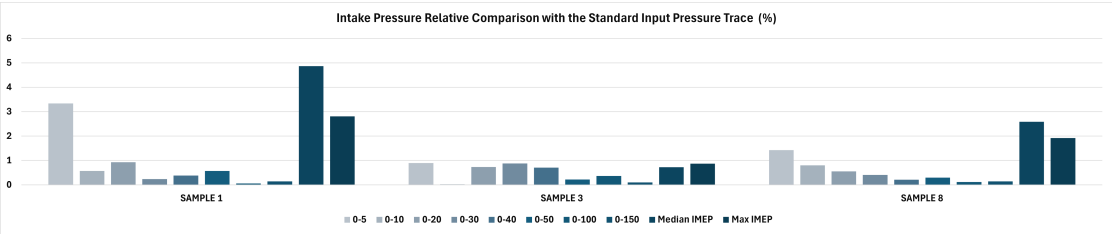

Figure 5.12: Intake Pressure Relative Comparison with the Standard Input Pressure Trace

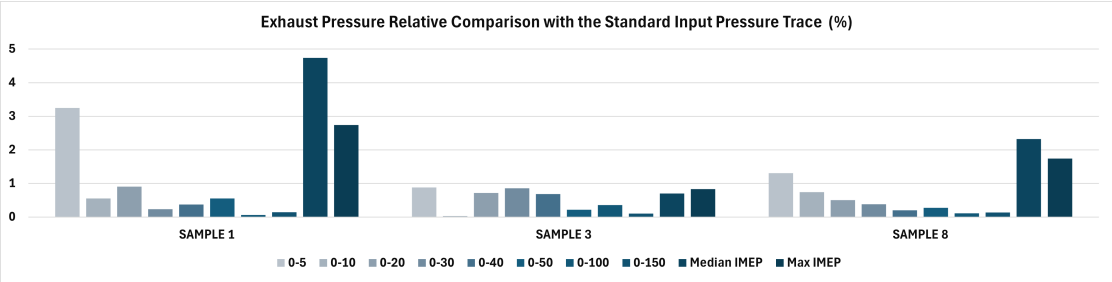

Figure 5.13: Exhaust Pressure Relative Comparison with the Standard Input Pressure Trace

An analysis of the sensitivity of boundary temperature conditions to the input pressure trace also showed minimal changes in boundary temperature outputs compared to the standard input. With the single pressure trace with median or maximum IMEP input producing a relative change of less than 1.5%, and by

averaging the cycle input over 10 or more cycles, the relative change is less than 0.5%.

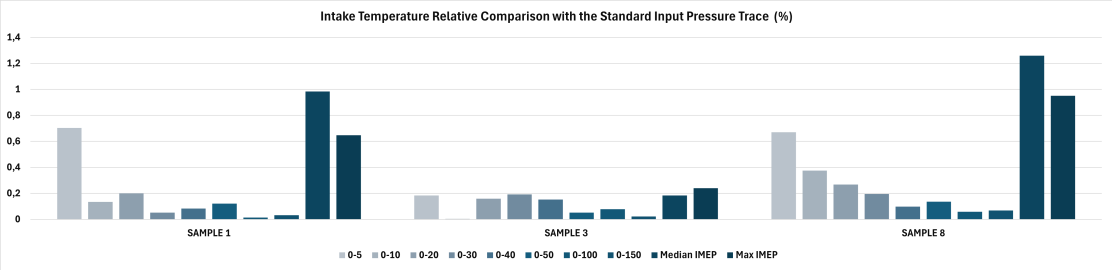

Figure 5.14: Intake Temperature Relative Comparison with the Standard Input Pressure Trace

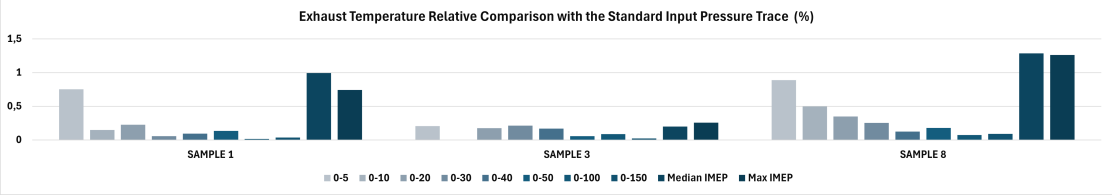

Figure 5.15: Exhaust Temperature Relative Comparison with the Standard Input Pressure Trace

Analysis of cumulative energy loss showed that averaging 10 or more cycles resulted in a relative change of less than 4%, while a single pressure trace with median or maximum IMEP input produced a relative change greater than 10%.

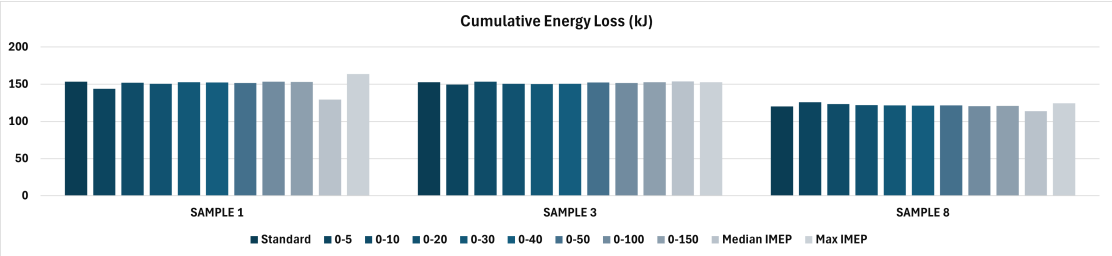

Figure 5.16: Cumulative Energy Loss output from the loop

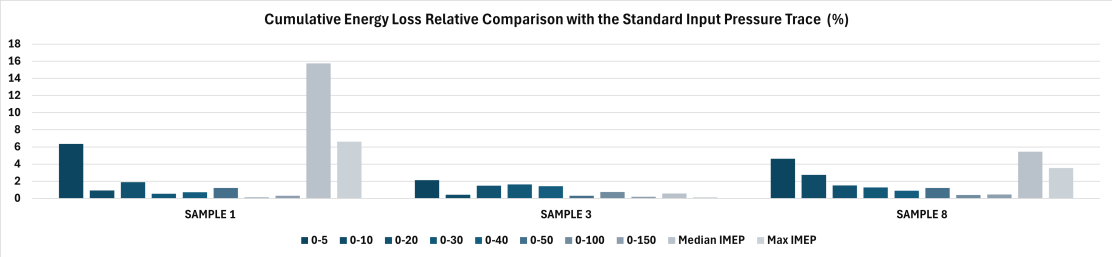

Figure 5.17: Cumulative Energy Loss Relative Comparison with the Standard Input Pressure Trace

Analysis of combustion phasing indicated that using a single pressure trace with median or maximum IMEP input resulted in a relative change greater than 60%. In contrast, averaging 40 or more cycles reduced the relative change to less than 20%. The relative change in combustion phasing showed a strong sensitivity to cycle-to-cycle variability, and it is probable that the relative change produced by the input ranges will vary depending on the coefficient of variation (CoV) and the operating conditions of the test run.

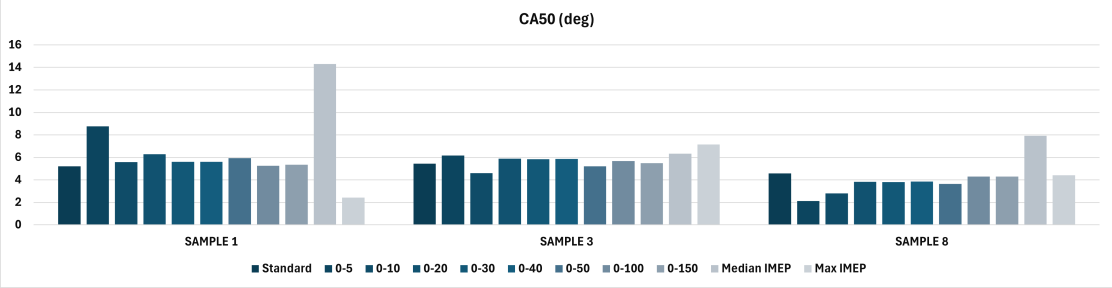

Figure 5.18: CA50 output from the loop

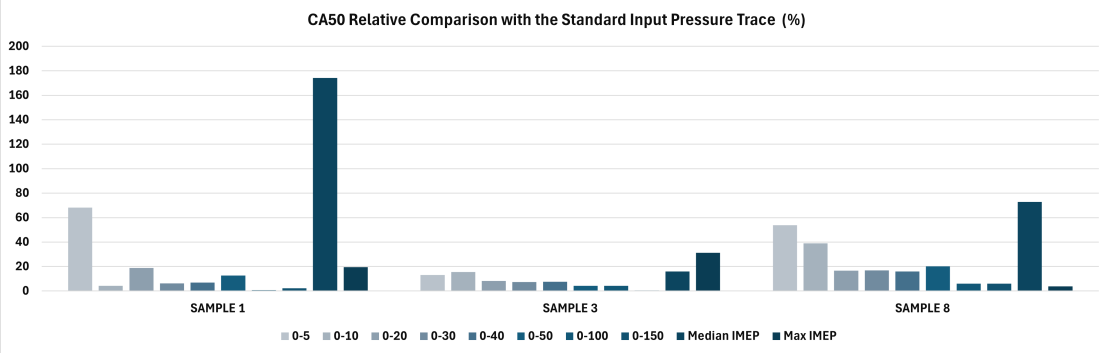

Figure 5.19: CA50 Relative Comparison with the Standard Input Pressure Trace

Analysis of burn duration indicated that using a single pressure trace with median or maximum IMEP input resulted in a relative change greater than 30%. In contrast, averaging 40 or more cycles reduced the relative change to less than 5%.

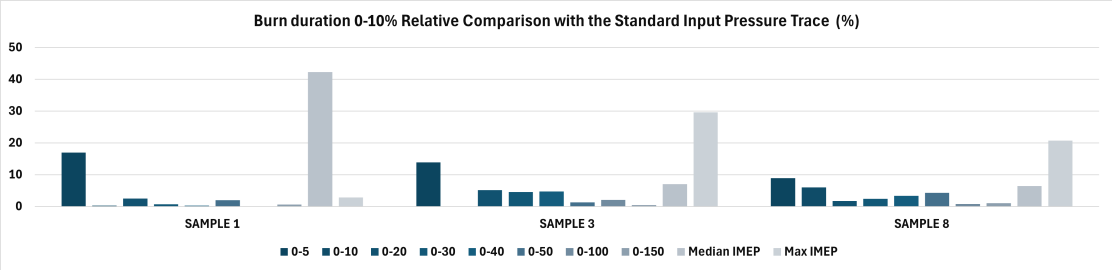

Figure 5.20: Burn Duration 0-10% Relative Comparison with the Standard Input Pressure Trace

5.3 Research Question 1.2: How well does the simulation MCE compare to experimental MCE data

Please refer to section 4.1.3; 4.1.6 and 4.3 for descriptions on the specific hardware differences between the models and engines.

This section discusses the findings relative to Research Question 1.2, specifically regarding the hardware discrepancies identified between the simulated environment and the experimental configurations. Rather than evaluating the correlations between the two domains, the results and discussion focuses on the points of divergence. This shift in focus is necessary to characterize the impact of geometric and structural variations (such as manifold architecture, cam shape, etc) on the resultant gas dynamics. By isolating these hardware-induced variances, the sensitivity of the 0D/1D model to physical deviations can be more accurately quantified.

The results demonstrate that the iterative loop - spanning from the physical SCE through the TPA to the virtual MCE - exhibits a high degree of accuracy. This correlation indicates that the simulation models are robustly tuned for the KIT SCE experimental setup. However, discrepancies are observed in the simulated MCE trace, particularly during the compression stroke, where we observe the simulated MCE overfitting the SCE and the TPA.

Observing the red curve, denoting the HYCET engines' experimental data, discrepancies are localized near Top Dead Center (TDC) and in the regions proximate to Inlet Valve Closing (IVC), Exhaust Valve Opening (EVO), and Bottom Dead Center (BDC). As illustrated in Figure 5.21, these deviations correspond to the commencement of the compression stroke and the concluding phases of the expansion stroke. The divergence in these specific regions suggests that the experimental engine has been built with an alternative cam profile - removing the validity of the comparison.

It was further observed that the experimental engine exhibits characteristic "bow-shaped" curve in figure 5.21 - during both the compression and expansion strokes. This phenomenon is likely attributable to transient heat transfer effects during the compression stroke, and a synergistic combination of heat loss and evolving gas composition during expansion. These factors dynamically influence the effective polytropic coefficient (n) of the charge and exhaust gases, resulting in the non-linear behavior observed in the figure. Consequently, the curvature reflects

the continuous variation of the polytropic index as a function of the instantaneous cylinder temperature and thermophysical gas properties. Furthermore, the base-

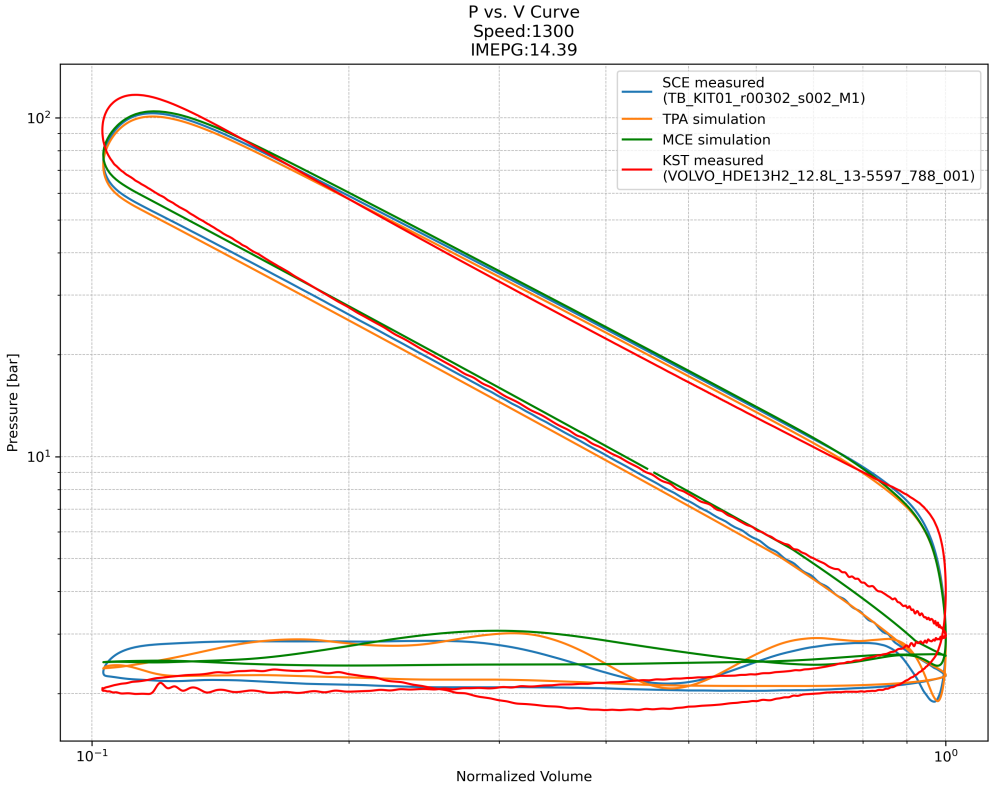

Figure 5.21: Log-P log-V diagram of the SCE, simulated TPA and MCE models and the experimental MCE data

line inlet manifold pressure and exhaust back-pressure configurations were found to be inconsistently calibrated between the two environments.

These findings further underscore the operational and hardware-level inconsistencies previously identified within the dataset. The resulting impact on the gas exchange process is clearly illustrated in the simplified pumping loop of the $\log(p) - \log(V)$ diagram (Figure 5.22). The divergence in the pumping loop area emphasizes the variation in the work required for induction and scavenging, highlighting the sensitivity of the iterative loop to valve timing and boundary pressure accuracy. Figure 5.23 illustrates that the inlet manifold pressures are distinctly different. The results indicate a higher boost pressure inherent to the experimental tests compared to the parameters configured in the simulation models. This discrepancy was, however, anticipated due to the independent nature of the experimental and numerical studies. The higher intake pressure in the SCE suggests

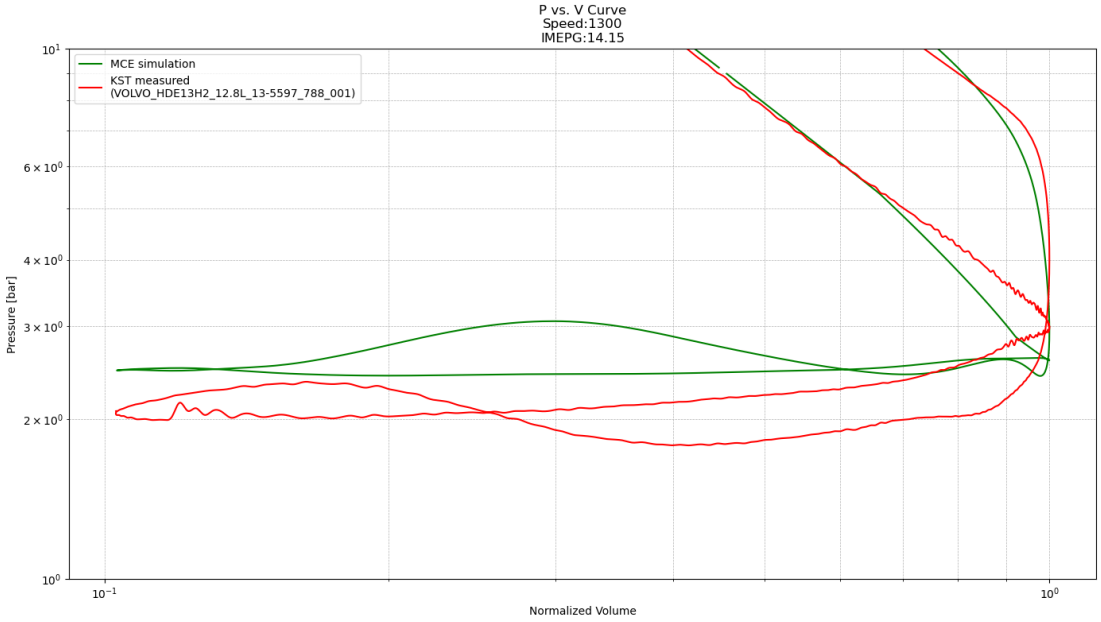

Figure 5.22: LogP-logV curve for the simulated and the experimental MCE systems

a greater charge density, which must be reconciled in the virtual MCE to ensure high-fidelity synchronization of the boundary conditions within the iterative loop.

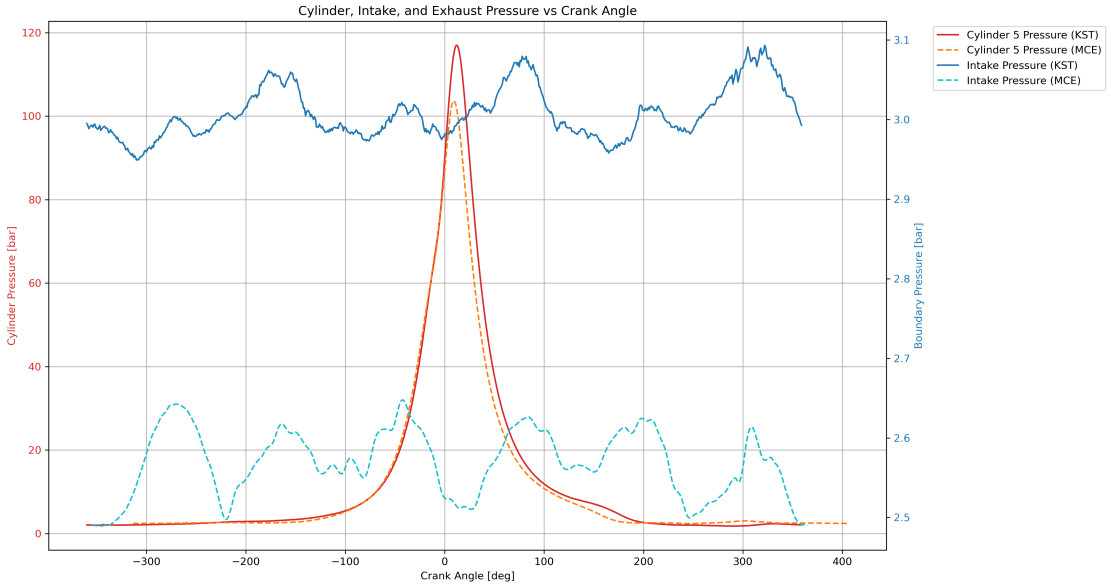

Figure 5.23: Pressure traces and inlet manifold pressures compared for the virtual and experimental MCE.

It was observed, however, that the increased boost pressure did not reflect in the volumetric efficiency metric presented in Figure 5.24. This suggests that the gas exchange systems in the simulation models possess a higher flow potential or represent a more optimized configuration than the experimental hardware.

This discrepancy is also reflected in the indicated efficiency metric described in Figure 5.25, where the experimental MCE is approximately 4 percentage points lower than the values recorded in any of the other Loop entities. Given the substantial divergence between the two setups, the systems are currently too dissimilar to draw definitive conclusions. Recommendations on the methodology required to normalize these parameters and proceed with the study are offered in the following section.

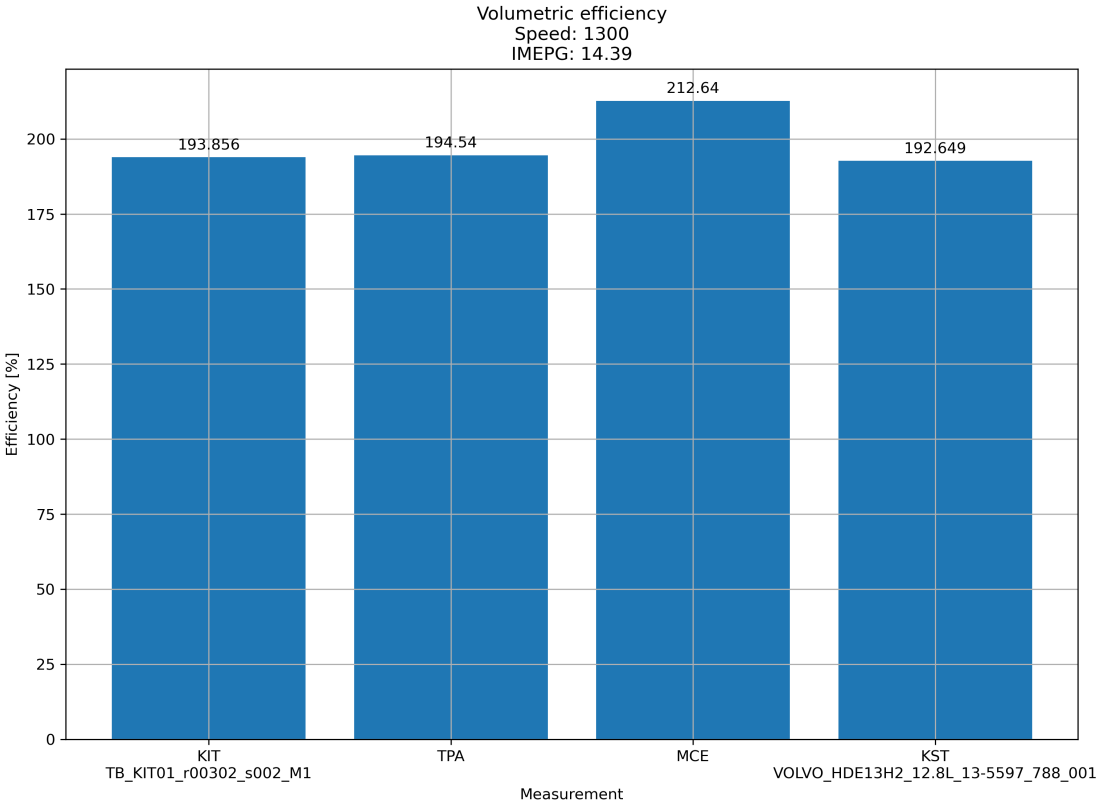

Figure 5.24: Volumetric Efficiency

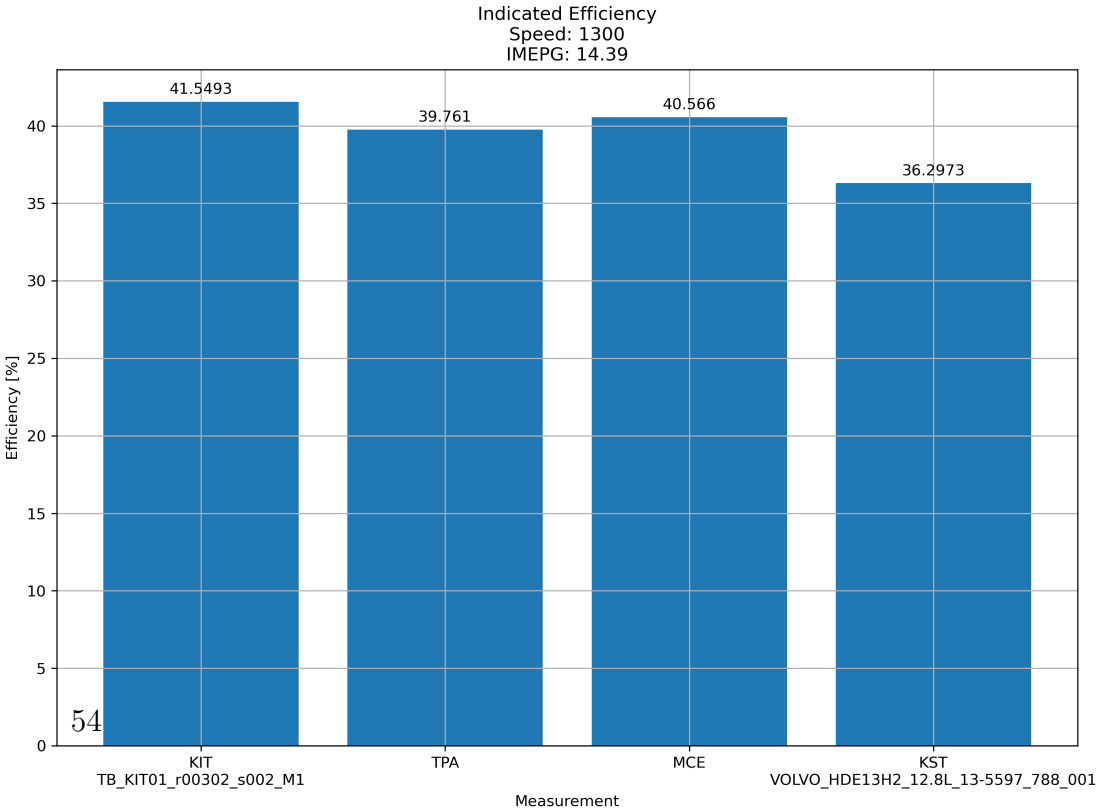

Figure 5.25: Indicated Efficiency

6
Conclusion

This research demonstrates significant potential as a novel development framework for MCE prototypes, which integrates empirical premixed hydrogen combustion data from a SCE test rig into a 0D/1D TPA model, which calculates a high resolution burn rate and then uses this burn rate as input into a detailed MCE simulation in GT-Suite. This methodology enables observation of a MCE within its system context while maintaining the resolution of a physics informed local combustion event.

However, due to the absence of a second iteration and the time scale of which a single iteration occupied in the closed loop system, this study was unable to generate a sufficient dataset to characterize the progression of near real time co-simulation, verify the precision of the resulting MCE output or justify the potential financial and productivity benefits possible. Furthermore, a direct validation of the 0D/1D-MCE model against existing multi-cylinder experimental data was precluded by disparities in the respective operational conditions and inherent differences in the cam profiles. To resolve these limitations, future work must incorporate synchronized experimental configurations and loading conditions, and full access to a dedicated SCE to realize complete loop convergence and system validation.

Regarding the processing of input data, this study highlights the risks of utilizing a single combustion cycle, even one representing the median or maximum $IMEP_n$, due to the stochastic nature of cyclic variations. Quantitative analysis revealed that a 5-cycle average resulted in absolute deviations of up to 3% in boundary temperatures, and 1.5% in both boundary pressures and indicated efficiency, when compared to a 200-cycle baseline. Given the profound impact of cyclic variations on combustion phasing, it is concluded that a minimum sample size of 50 averaged cycles is required as a simulation input to ensure statistical significance and model stability - an important observation in the pursuit of realizing a near real time HiL system.

7

Discussion

7.1 Limitations

During the course of the project strict limitation hindered the full realization outlined by the project aim (see Section 1.2). This section aims to describe these limitation and highlight how they affect the project.

7.1.1 Engine Access

Initially, the experimental phase of this project was centered on a single-cylinder research engine at Chalmers University of Technology. This platform was derived from a 13L heavy-duty truck engine specifically configured for pre-mixed hydrogen combustion research. However, during the implementation phase, a critical malfunction rendered the engine inoperable.

The unavailability of the Chalmers engine presented a significant challenge for the operational validation of the data exchange interface. Without a functional test rig, the closed-loop synchronization between the physical hardware and the numerical models could not be fully realized in a real-time experimental context.

To mitigate these limitations and ensure a robust validation of the integrated framework, the project's scope was redirected to utilize the KIT SCE platform. This transition allowed for the utilization of high-fidelity experimental data to validate the communication and logic of the loop, as described in the preceding sections. Making this change only allowed for an initial loop simulation without any further iteration.

7.1.2 Data Availability

A significant advantage of the KIT SCE was the availability of a comprehensive experimental database that closely corresponded to its MCE counterpart—a capability that was lacking in the Chalmers engine platform. However, the integration of these two distinct datasets required a rigorous filtering process to ensure physical and thermodynamic consistency.

The scope of this comparative analysis was constrained by discrepancies in the operational envelopes; specifically, the KIT SCE and the HYCET MCE were originally tested at inconsistent engine speeds and load points. This misalignment necessitated the selection of a restricted subset of data. Ultimately, three KIT SCE datasets from "run-in" program tests were identified as the most viable candidates for comparison.

Further analysis revealed only two MCE datasets that provided a sufficient correlation to these SCE benchmarks, highlighting the inherent inconsistencies between the independent testing campaigns. Figure 7.1 illustrates the datasets exhibiting the highest degree of correlation between the KIT SCE and the HYCET MCE, which serve as the baseline for the comparative analysis presented in the following results section.

These data sets were simulated in the Loop following the process outlined by Figure 4.1. Considering the limitation described above, only an initial loop iteration was possible; the results are therefore not converged. This process forms the basis for further development, and the results should be considered an initial proof of concept.

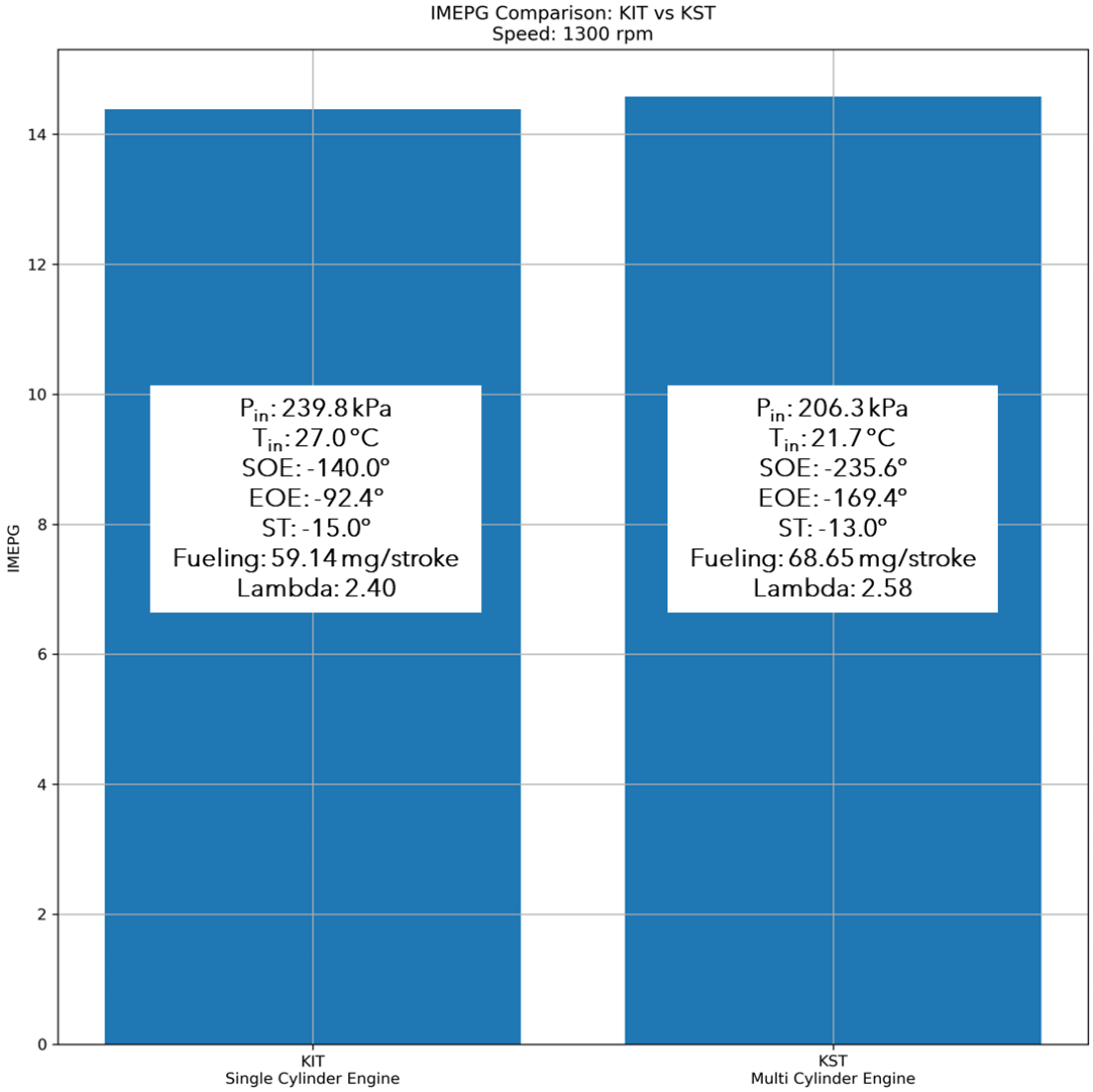

Figure 7.1: SCE and MCE datasets that showed the best agreement used for comparison

7.2 Recommendations

To enhance the fidelity or the operation fidelity of the developed system, several important refinements are recommended. Firstly, it is imperative to achieve full closed loop numerical convergence using a load point and operating condition already established within the KST engine dataset corresponding to a build with the same cam profile installed; this will serve as the definitive validation for the virtual MCE concept model and also the functional value of The Loop as an engineering tool.

Secondly, the computational, data handling and system operations framework should migrate toward a more robust architecture. Transitioning to a Linux-based environment and adopting more precise programming languages, such as C, in place of the current Python-based scripts would significantly improve processing time, computation speeds and adherence to well developed software engineering standards. This transition should be coupled with the development of a graphical user interface (GUI) to improve usability for the engineer and the test rig operator.

Furthermore, regarding the physical accuracy of the model, the current square wave injector approximation should be replaced with a more comprehensive and realistic modeling strategy for better characterization of the induction process. Additionally, the 0D/1D models require a comprehensive calibration phase specifically targeting heat transfer coefficients and mechanical friction sub-models to reconcile the efficiency discrepancies noted in this study.

A significant area for future research involves the investigation of Fast Running Models (FRM) and xRT solver technologies, available through GT software packages. Technical literature suggests that xRT models facilitate rapid simulation times, potentially enabling real-time "Hardware-in-the-Loop" (HiL) applications where the virtual MCE converges with marginal latency relative to the physical SCE [2]. While these methods will involve a trade off in model fidelity, simulation speed is critical for near real time MCE modeling. These models were also recommended in previous research [7], while using a MATLAB Simulink, FRM has also proven to be an effective means of dealing with prolonged simulation times [16].

Finally, the dedication of a specific SCE test bed to this tool is proposed. Since The Loop is platform independent requiring only a corresponding MCE model for any given combustion system. A dedicated setup would allow for comprehensive testing of convergence stability and the underlying system sensitivities. Enabling this dedicated environment would act as a catalyst for validating the transition

to FRM and xRT modeling methods, ultimately maturing the system into a high-performance engine development tool.

References

[1] Shitu Abubakar et al. "Recent progress on hydrogen-fueled port fuel injection spark ignition engine: A systematic review". In: *Thermal Science* 29 (5 Part A 2025), pp. 3509–3528. ISSN: 0354-9836. DOI: 10.2298/tsci240930081a.

[2] André Ahlskog et al. *Operating a Single-Cylinder Engine with a Multi-Cylinder Engine 1D-Model in the Loop with Real-Time Combustion Feedback*. Wärtsilä Technical Presentation Materials. Presented on October 09, 2023. Oct. 2023.

[3] Naqash Azeem et al. "Experimental study of cycle-by-cycle variations in a spark ignition internal combustion engine fueled with hydrogen". In: *International Journal of Hydrogen Energy* 60 (Mar. 2024), pp. 1224–1238. ISSN: 03603199. DOI: 10.1016/j.ijhydene.2024.02.182.

[4] Thomas Gal et al. "Modeling of Hydrogen Combustion from a 0D/1D Analysis to Complete 3D-CFD Engine Simulations". In: *Energies* 17.22 (2024), pp. 1–18. DOI: 10.3390/en17225543.

[5] Gamma Technologies. *Engine Performance Application Manual*. Version 2024. Gamma Technologies. Westmont, IL, 2024.

[6] John B.. Heywood. *Internal combustion engine fundamentals*. McGraw-Hill Book Company, 1988, p. 930. ISBN: 007028637X.

[7] Karthik Hitavalli Prakash and Rushi Kiran Vangala. "Online Closed Loop Combustion Analysis of Compressed Ignition Engines". Master's Thesis in Automotive Engineering. Göteborg, Sweden: Chalmers University of Technology, 2017.

[8] *Internal combustion engines — Determination and method for the measurement of engine power — General requirements*. Standard ISO 15550:2016. Geneva, CH: International Organization for Standardization, 2016.

[9] G. A. Karim. "Hydrogen as a spark ignition engine fuel". In: *International Journal of Hydrogen Energy* 28.5 (2003), pp. 569–577. DOI: 10.1016/S0360-3199(02)00150-7.

[10] Hjalmar Lindqvist and Petter Overby. *A Literature Review of Hydrogen Internal Combustion Engines: An Evaluation of Recent Developments and Challenges*. Tech. rep. Accessed: 2025-05-15. Chalmers University of Technology, 2024. URL: https://www.chalmers.se.

[11] A. J. Martyr, M. A. Rogers, and M. A. Plint. *Engine Testing: The Design, Building, Modification and Use of Powertrain Test Facilities*. 4th. ProQuest Ebook Central. Elsevier Science & Technology, 2012. Chap. 1. URL: http://ebookcentral.proquest.com/lib/chalmers/detail.action?docID=872579.

[12] Ojo Emmanuel Olufisayo, Freddie Liswaniso Inambao, and Riaan Stopforth. *GT-Power for Internal Combustion Engine Simulation: A Review*. Tech. rep. 2025, pp. 1001–4055.

[13] Reza Rezaei et al. "Numerical and Experimental Investigations of Hydrogen Combustion for Heavy-Duty Applications". In: *SAE Technical Papers* 2021 (2021). DOI: 10.4271/2021-01-0522.

[14] Robert W Schefer, Christopher White, and Jay Keller. *CHAPTER 8-LEAN HYDROGEN COMBUSTION*. Tech. rep.

[15] S. Shahpouri et al. *Hydrogen-Fueled Internal Combustion Engines: 0D Modeling and Experimental Validation*. Tech. rep. Presented at the Combustion Institute-Canadian Section Spring Technical Meeting. University of Ottawa, 2023.

[16] Ben Smulter. "Building a GT-Power-in-the-Loop System comprising a Fast-Running Model as an Extended Digital Twin for a Single-Cylinder Research Engine". Master's Thesis in Energy and Information Technology. University of Vaasa, 2024.

[17] Sebastian Verhelst, Roger Sierens, and Stefaan Verstraeten. "A Critical Review of Experimental Research on Hydrogen Fueled SI Engines". In: *SAE Transactions*. Section 3: Journal of Engines 115 (2006), pp. 264–274. URL: https://www.jstor.org/stable/44687302.

[18] C. M. White, R. R. Steeper, and A. E. Lutz. "The hydrogen-fueled internal combustion engine: a technical review". In: *International Journal of Hydrogen Energy* 31 (10 Aug. 2006), pp. 1292–1305. ISSN: 03603199. DOI: 10.1016/j.ijhydene.2005.12.001.

[19] Feng Zhou et al. "Abnormal combustion and NOx emissions control strategies of hydrogen internal combustion engine". In: *Renewable and Sustainable Energy Reviews* 219 (2025), p. 115847. DOI: 10.1016/j.rser.2024.115847.

A

Appendix 1: Supplementary Plots for Research Question 1.1

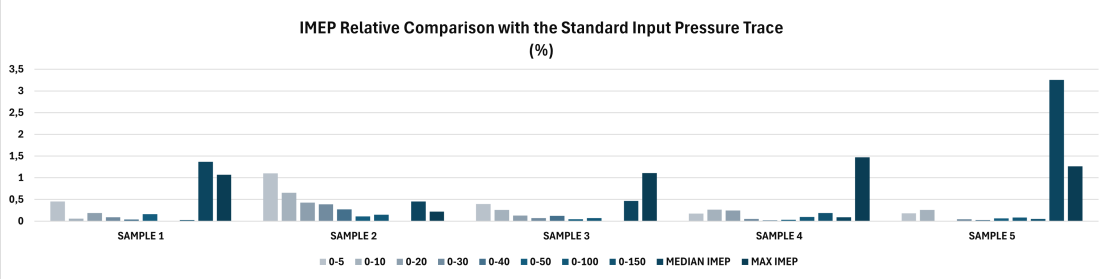

Figure A.1: IMEP Relative Comparison with the Standard Input Pressure Trace

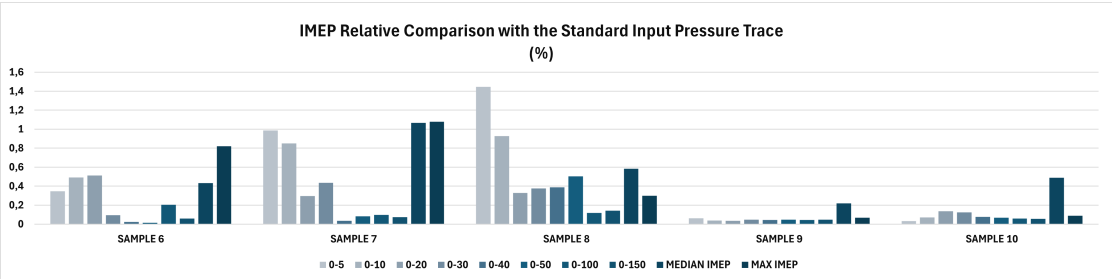

Figure A.2: IMEP Relative Comparison with the Standard Input Pressure Trace

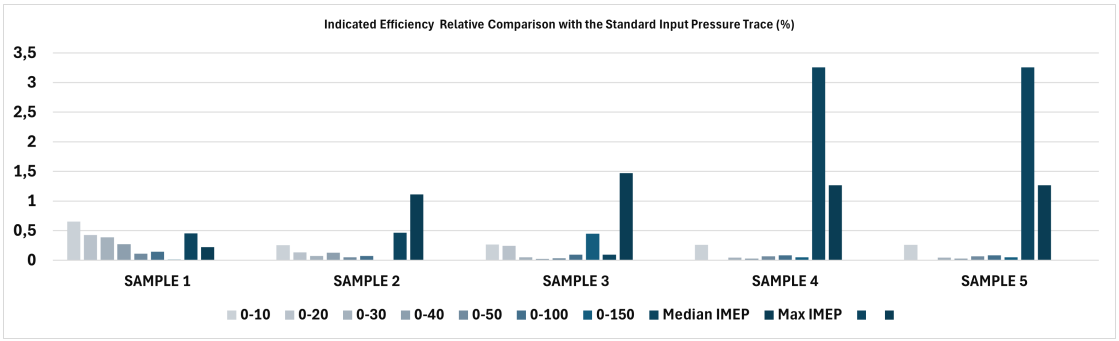

Figure A.3: Indicated Efficiency Relative Comparison with the Standard Input Pressure Trace

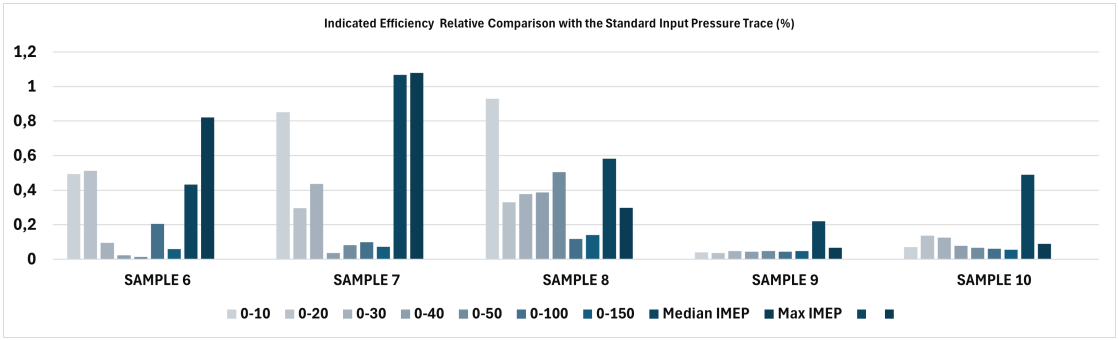

Figure A.4: Indicated Efficiency Relative Comparison with the Standard Input Pressure Trace

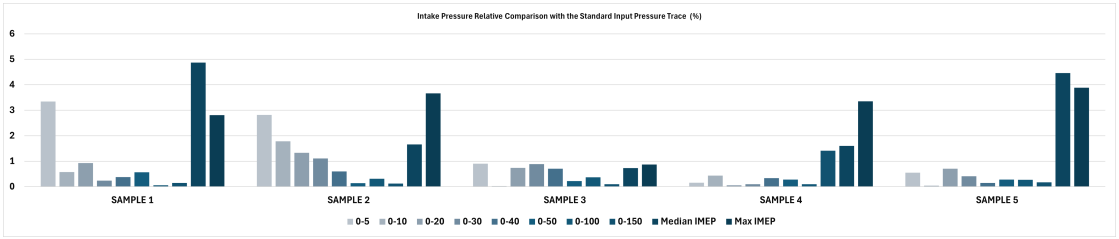

Figure A.5: Intake Pressure Relative Comparison with the Standard Input Pressure Trace

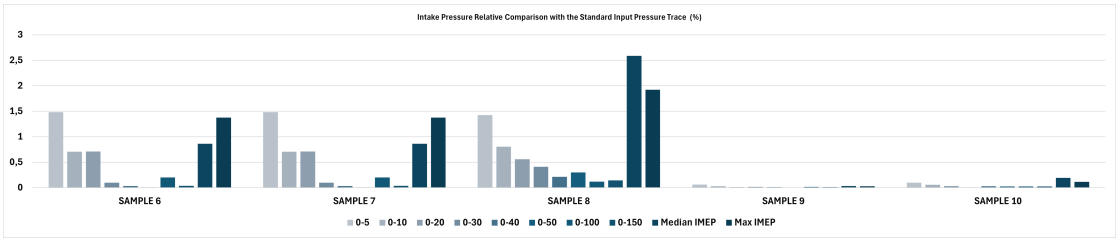

Figure A.6: Intake Pressure Relative Comparison with the Standard Input Pressure Trace

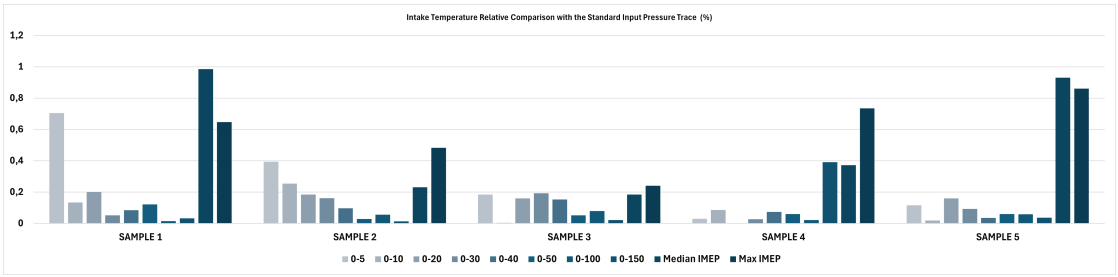

Figure A.7: Intake Temperature Relative Comparison with the Standard Input Pressure Trace

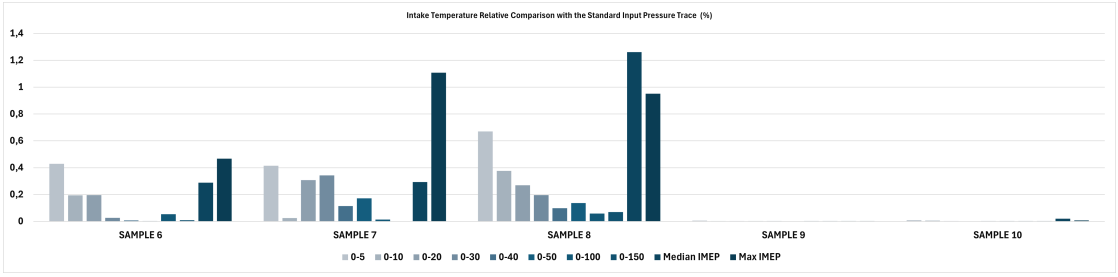

Figure A.8: Intake Temperature Relative Comparison with the Standard Input Pressure Trace

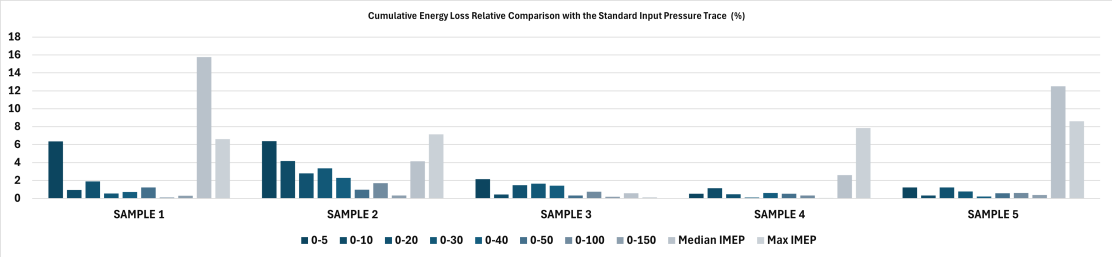

Figure A.9: Energy Loss Relative Comparison with the Standard Input Pressure Trace

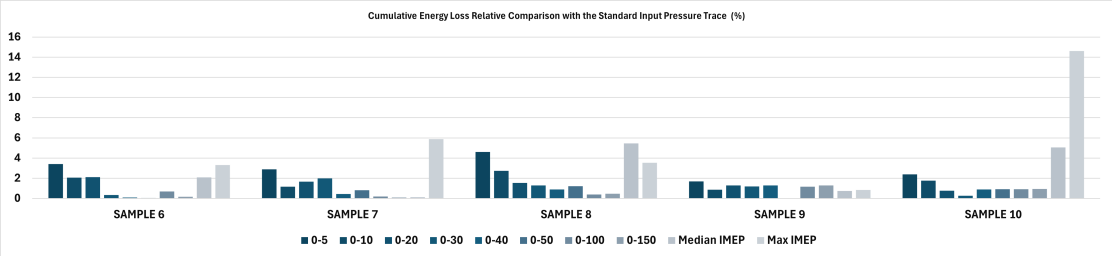

Figure A.10: Energy Loss Relative Comparison with the Standard Input Pressure Trace

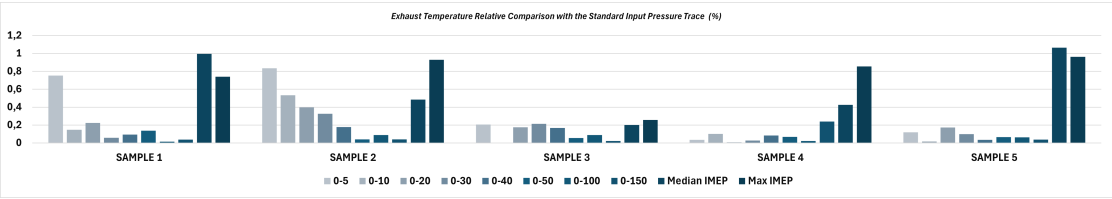

Figure A.11: Exhaust Temperature Relative Comparison with the Standard Input Pressure Trace

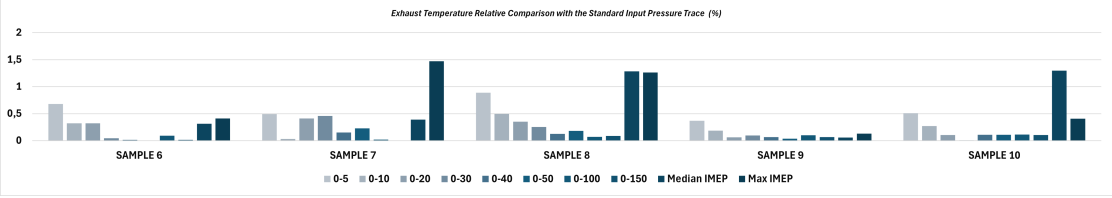

Figure A.12: Exhaust Temperature Relative Comparison with the Standard Input Pressure Trace

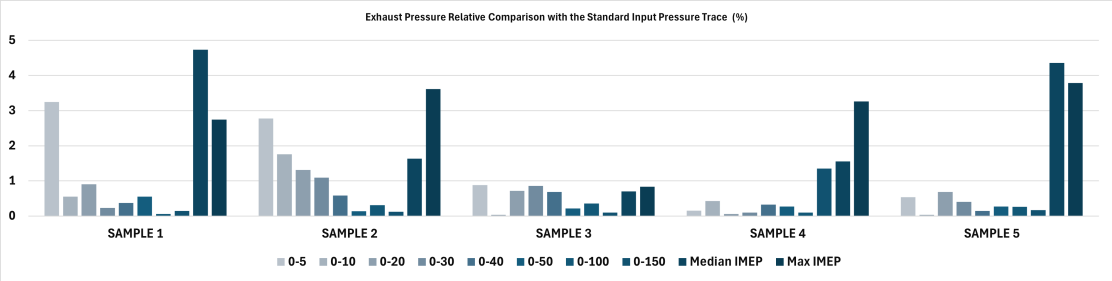

Figure A.13: Exhaust Pressure Relative Comparison with the Standard Input Pressure Trace

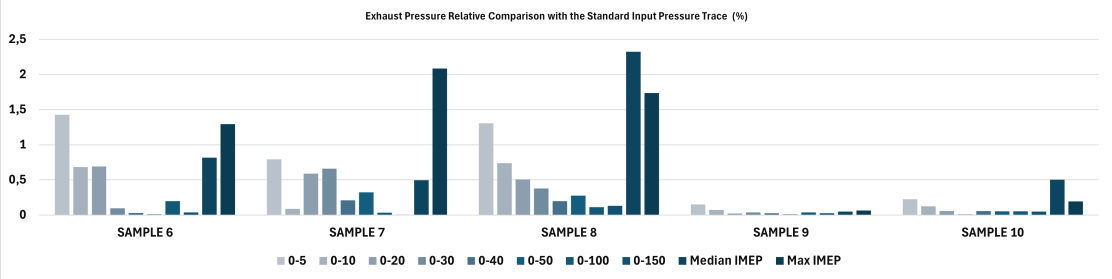

Figure A.14: Exhaust Pressure Relative Comparison with the Standard Input Pressure Trace

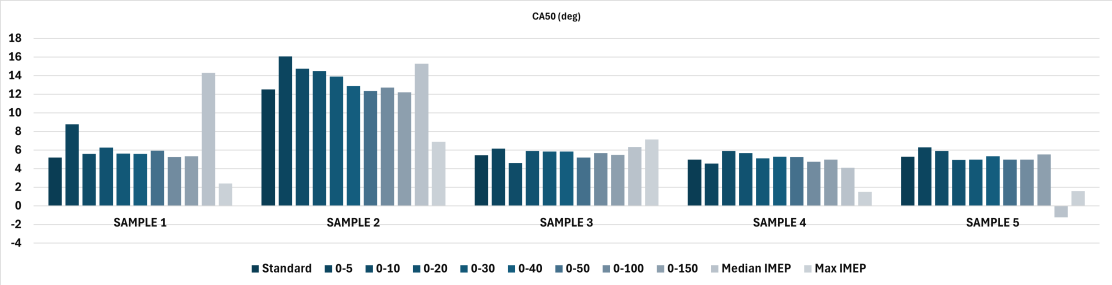

Figure A.15: CA50 output from the loop

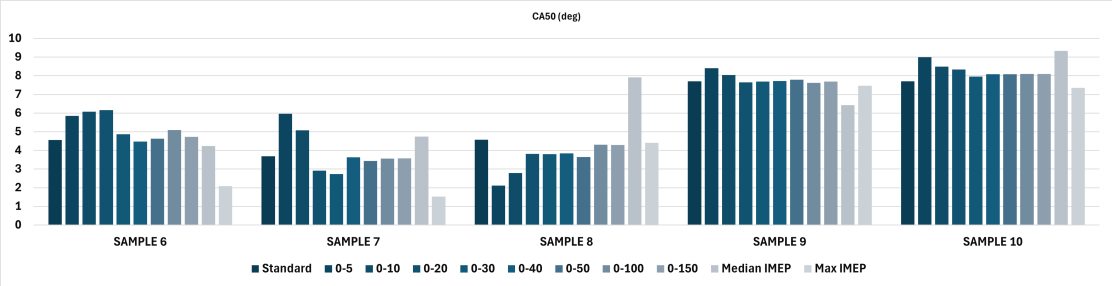

Figure A.16: CA50 output from the loop

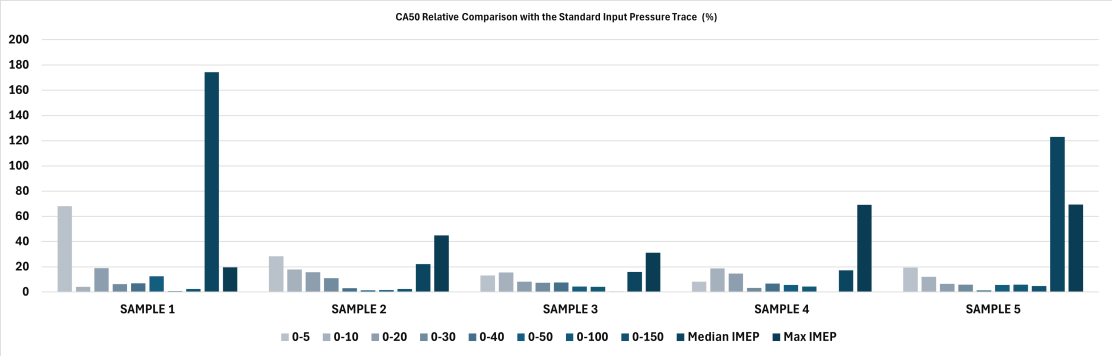

Figure A.17: CA50 Relative Comparison with the Standard Input Pressure Trace

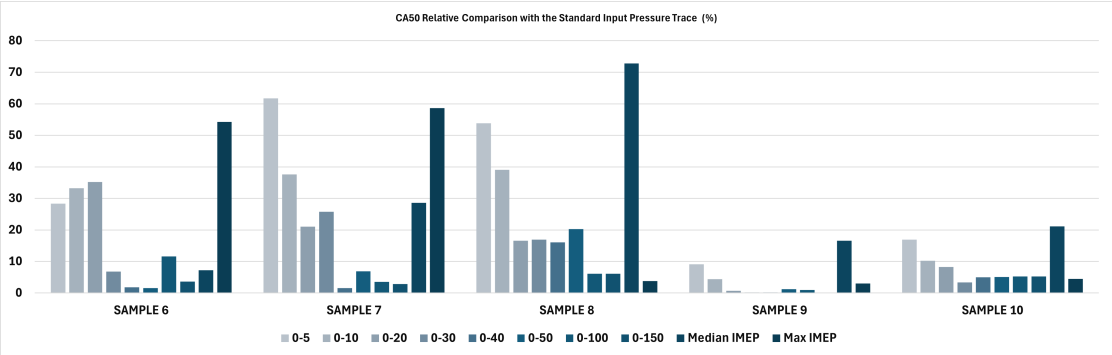

Figure A.18: CA50 Relative Comparison with the Standard Input Pressure Trace

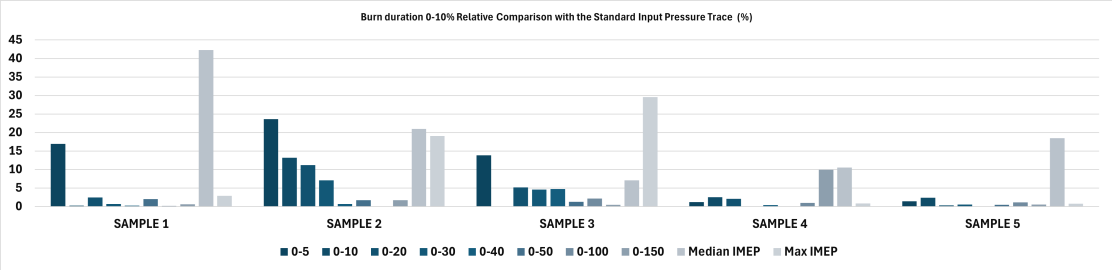

Figure A.19: Burn Duration 0-10% Relative Comparison with the Standard Input Pressure Trace

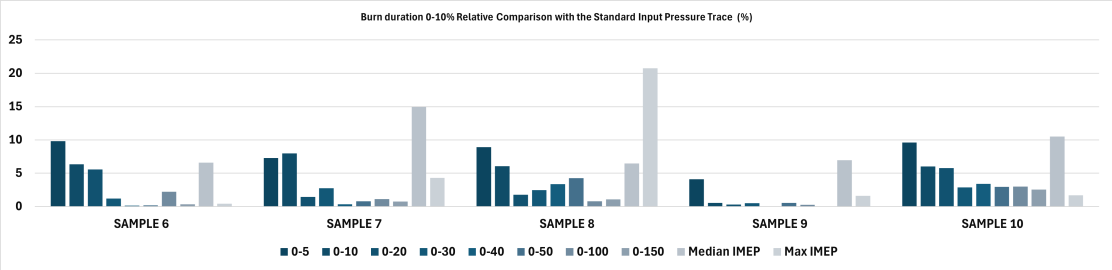

Figure A.20: Burn Duration 0-10% Relative Comparison with the Standard Input Pressure Trace

B

Appendix 2: Effects of the Connecting Rod Length

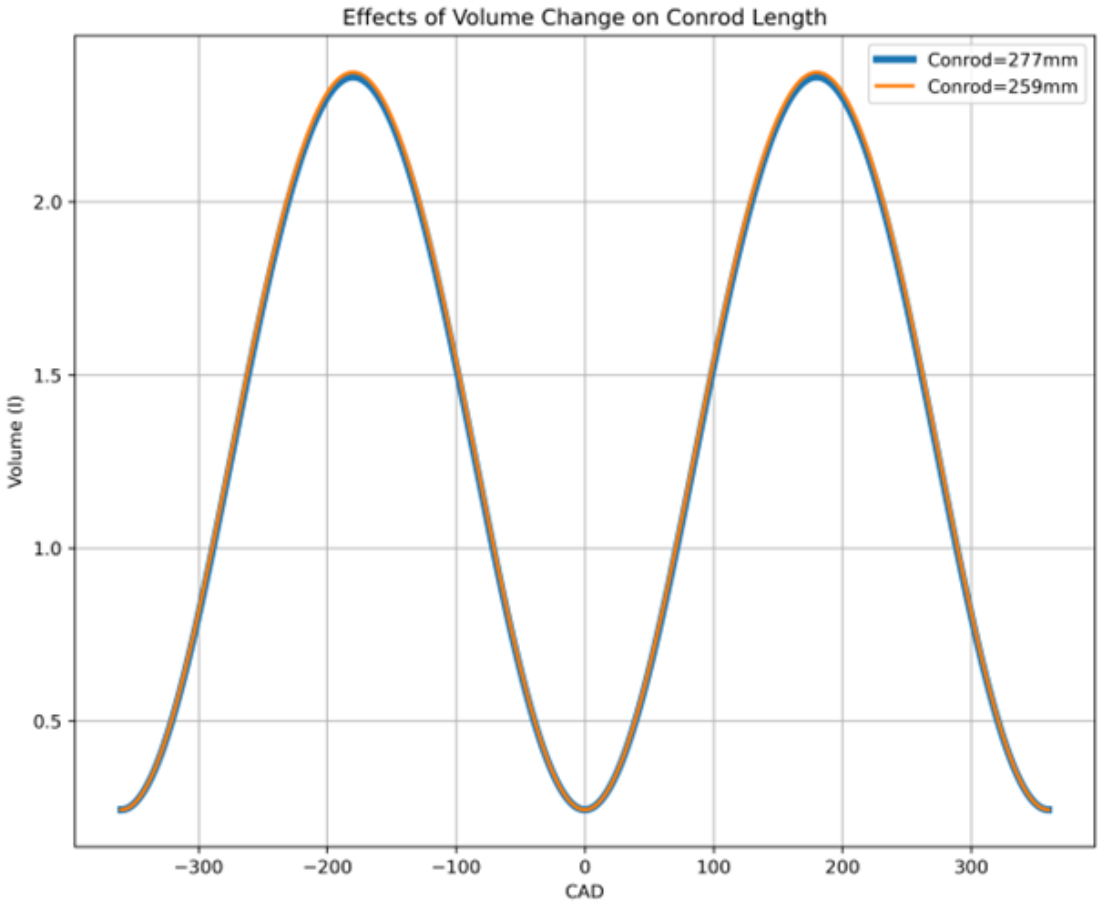

Figure B.1: Comparison of the conrod length of the MCE (259 mm) to the conrod length of the KIT SCE (277 mm) on the combustion cycle pressure curve

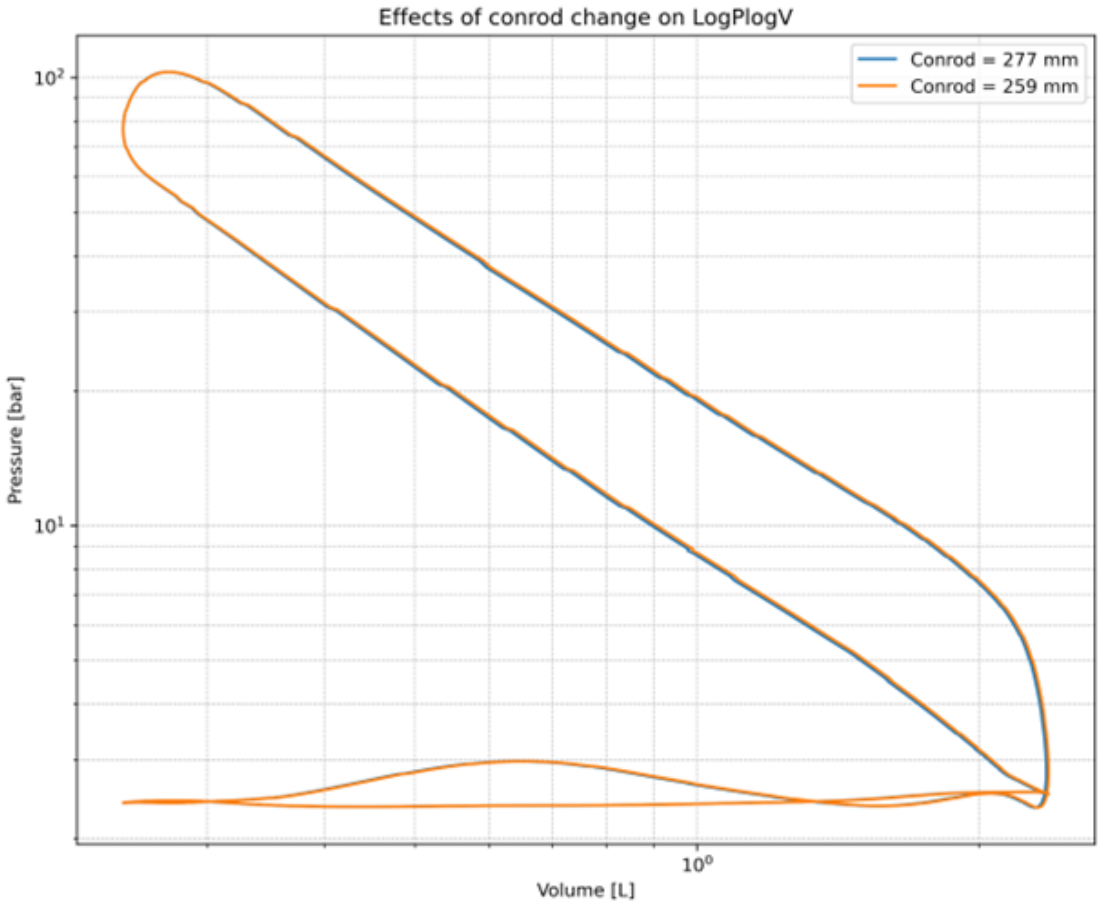

Figure B.2: Comparison of the conrod length of the MCE (259 mm) to the conrod length of the KIT SCE (277 mm) on a LogP-LogV curve.

C

Appendix 3: MCE knock filtering and error checks

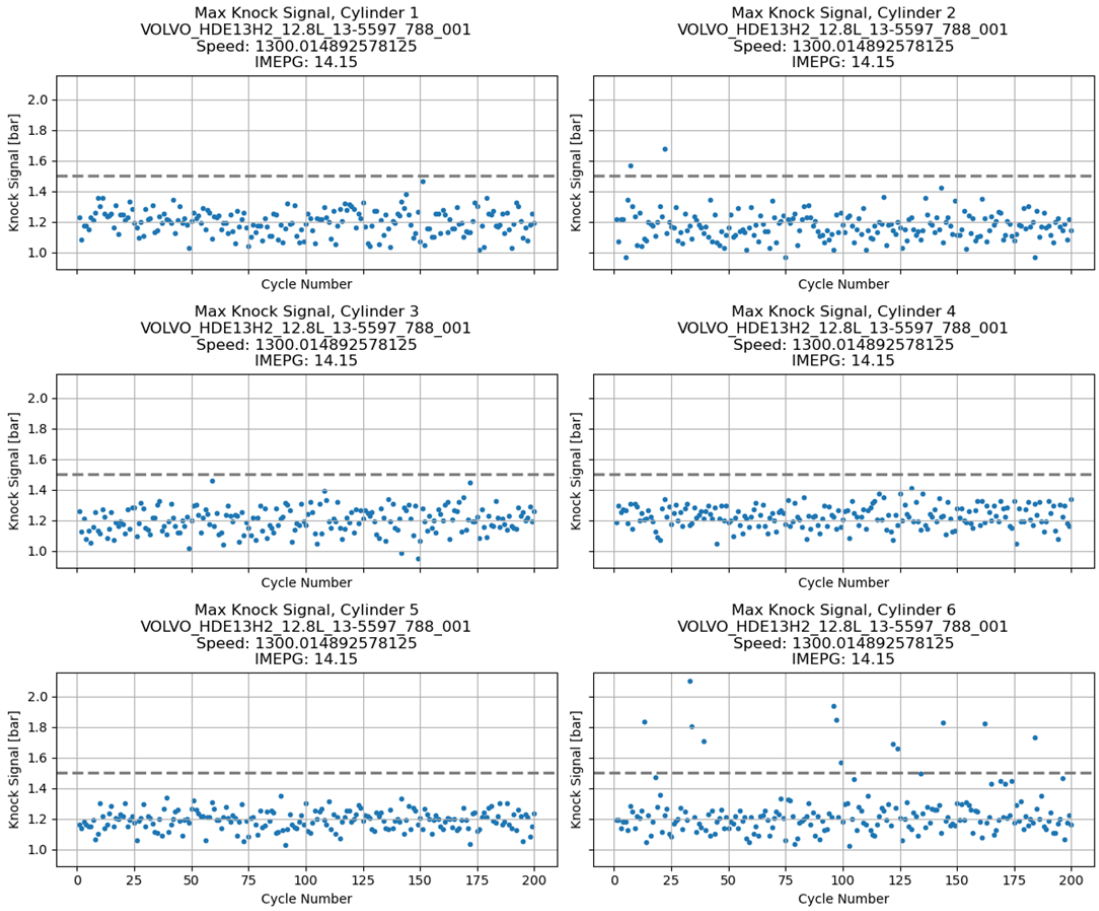

Figure C.1: Maximum knock amplitude with a 1.5 bar knock filter applied to the experimental MCE data.

Figure C.1 shows a 1.5 bar knocking threshold applied to the maximum knock amplitude of data extracted from a high pass filter of each cylinder in the MCE. Cylinders 2 and 6 had cycles which fell outside of the knock threshold.

Figure C.2, shows the pressure traces of these knocking cycles and it was found that the knock in cylinder 6 was causing thermal shock on the in-cylinder pressure sensor - resulting in the observed sensor drift in figure C.3.

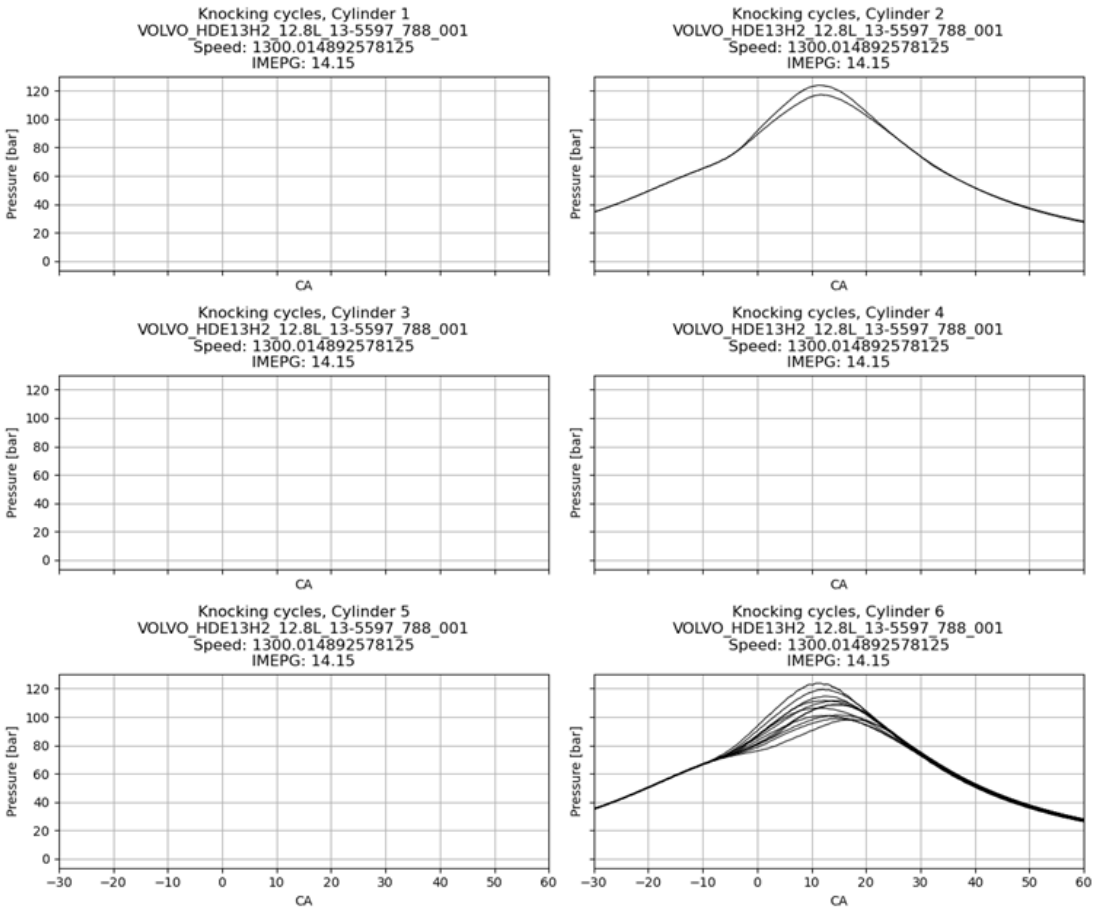

Figure C.2: Knocking pressure traces filtered from each cylinder which were outside of the knock threshold

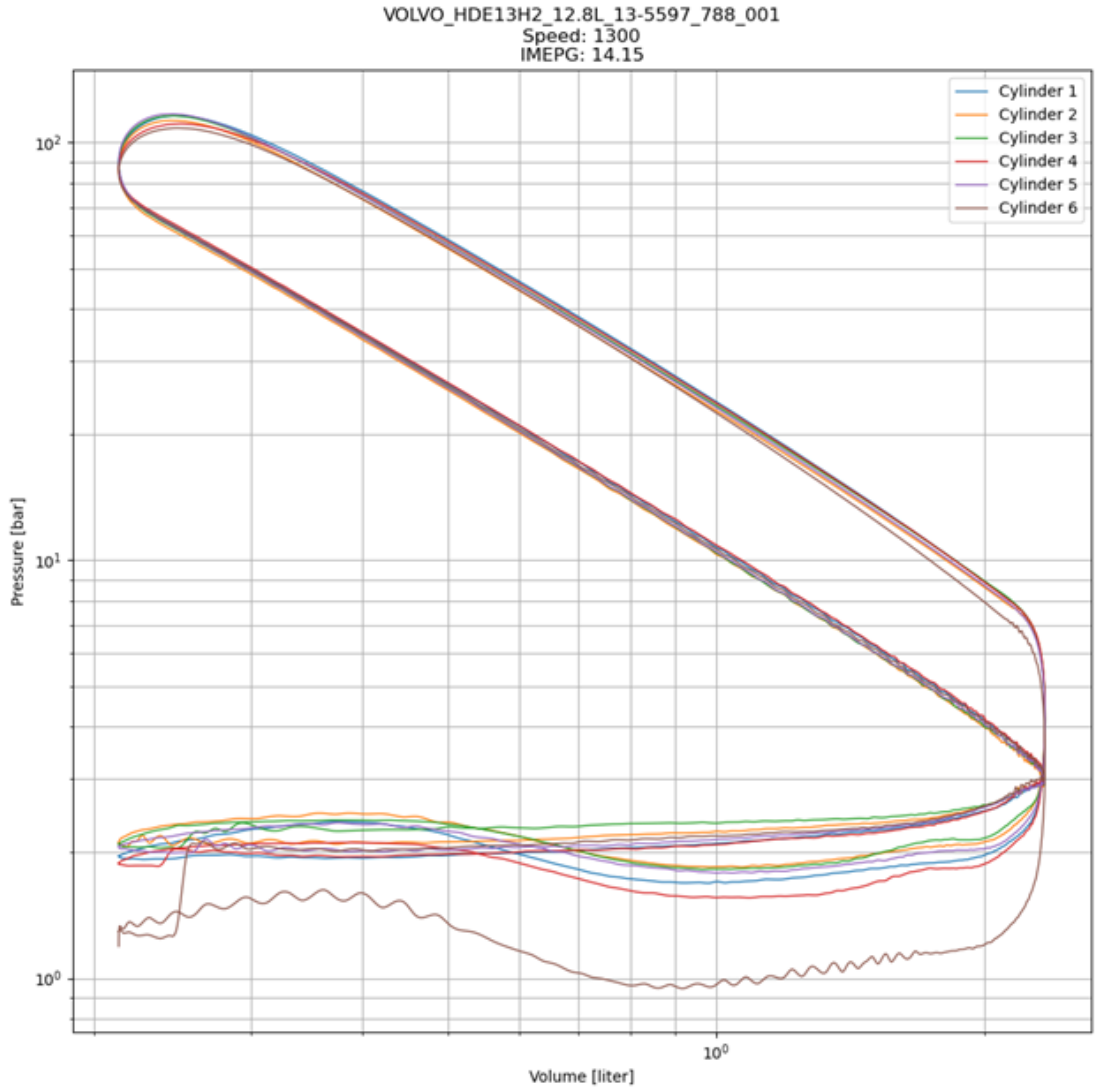

Figure C.3: Average in-cylinder pressure of each cylinder plotted on a LogP-LogV diagram.

DEPARTMENT OF SOME SUBJECT OR TECHNOLOGY
CHALMERS UNIVERSITY OF TECHNOLOGY
Gothenburg, Sweden
www.chalmers.se

CHALMERS
UNIVERSITY OF TECHNOLOGY